SAND--90-2009

SAND90-2009
Unlimited Release
Printed November 1990

DE91 006428

PREDICTIVE AGING RESULTS FOR CABLE MATERIALS IN NUCLEAR POWER PLANTS

Kenneth T. Gillen and Roger L. Clough
Sandia National Laboratories
Albuquerque, NM 87185

ABSTRACT

In an earlier report, we derived a time-temperature-dose rate superposition methodology, which, when applicable, can be used to predict cable degradation versus dose rate, temperature and exposure time. This methodology results in predictive capabilities at the low dose rates and long time periods appropriate to ambient nuclear power plant environments. The methodology was successfully applied to several polymeric cable materials and then verified for two of the materials by comparisons of the model predictions with 12 year, low-dose-rate aging data on these materials from a nuclear environment. In this report, we provide a more detailed discussion of the methodology and apply it to data obtained on a number of additional nuclear power plant cable insulation (a hypalon, a silicone rubber and two ethylene-tetrafluoroethylenes) and jacket (a hypalon) materials. We then show that the predicted, low-dose-rate results for our materials are in excellent agreement with long-term (7 to 9 year), low dose-rate results recently obtained for the same material types actually aged under nuclear power plant conditions. Based on a combination of the modelling and long-term results, we find indications of reasonably similar degradation responses among several different commercial formulations for each of the following "generic" materials: hypalon, ethylene-tetrafluoroethylene, silicone rubber and PVC. If such "generic" behavior can be further substantiated through modelling and long-term results on additional formulations, predictions of cable life for other commercial materials of the same generic types would be greatly facilitated. Finally, to aid utilities in their cable life extension decisions, we utilize our modelling results to generate lifetime prediction curves for the materials modelled to date. These curves plot expected material lifetime versus dose rate and temperature down to the levels of interest to nuclear power plant aging.

TABLE OF CONTENTS

ACKNOWLEDGMENTS

This work was sponsored by the U.S. Department of Energy as part of their Plant Lifetime Improvement Program under the direction of D. L. Harrison. Their support is gratefully acknowledged. Able technical assistance was provided by P. D. Silva and G. M. Malone. We also thank L. D. Bustard for several useful suggestions and comments.

INTRODUCTION

Large quantities of electrical cables are present in nuclear power plants. Historical operational experience as well as research results suggest that nuclear safety-related cable insulation and jacket materials will gradually embrittle as they age under the influence of the relatively low-level radiation and elevated temperature operating conditions. Severe cable embrittlement might lead to cable failure in several ways. For example,

1) significantly embrittled cable might crack during maintenance activities if severely flexed.
2) embrittlement during aging might be enhanced during accident conditions, leading to failure.

Hence, it is important that life prediction tools be available to estimate the extent of cable embrittlement for specified thermal and radiation aging conditions.

Historical practice for estimating cable embrittlement is to use the Arrhenius equation for predicting cable performance in a thermal environment and the equal-dose, equal-damage assumption for predicting cable performance in a radiation environment. [1,2] When attempting to simulate a combined radiation plus thermal environment, life endurance estimates have traditionally been based on a sequential application of thermal and radiation exposures.

As noted in the literature, [1,2] the historical approach does not account for the possible presence of dose-rate or synergistic effects. Hence, it is desirable that a tool be developed that explicitly accounts for such "combined-environments" effects.

In an earlier report, we derived a time-temperature-dose rate superposition methodology, which, when applicable, can be used to make predictions on cable degradation versus dose rate, temperature and exposure time. [3] This methodology results in quantitative predictive capabilities at the low, experimentally inaccessible dose rates appropriate to ambient nuclear power plant environments. The methodology was successfully applied to combined radiation-thermal accelerated aging results for three cable jacketing materials (a neoprene, a hypalon and a PVC) and two cable insulation materials (a chemically cross-linked polyethylene and a low density polyethylene), allowing predictions to be made under typical nuclear power plant aging conditions.

In this report, we provide a more detailed discussion of the methodology and apply it to additional nuclear power plant cable materials, including another hypalon jacket and a number of additional insulation materials- a hypalon, a silicone rubber and two ethylene-tetrafluoroethylenes (ETFE). The results yield predictive capabilities under dose-rate and temperature conditions characteristic of operating nuclear power plants. We then show that the predicted results for our hypalon, silicone, ETFE and PVC materials are in excellent agreement with long-term (7 to 9 year), low dose-rate results recently obtained

for the same material types actually aged under nuclear power plant conditions. In addition, we provide life prediction information for all materials examined to date in a format that is useful to utilities as they make cable life extension decisions.

EXPERIMENTAL

MATERIALS

The materials for this study were carefully stripped, before aging, from low-voltage electrical cables used in nuclear power plant applications. Table 1 gives descriptions of the materials used in the present study (top 5 in Table) as well as the materials previously examined [3] together with abbreviations that will be utilized throughout this report. The insulation samples were aged as tubes, whereas the hypalon jacket was aged as a slit tube.

AGING PROCEDURES

Combined radiation-thermal exposures were carried out in an underwater cobalt-60 aging facility using water-tight aging cans (volume of ~ 1 liter), an arrangement that facilitated long-term exposures. Available dose rates ranged from ~10 Gy/h to 5×10^3 Gy/h (1 krad/h to 500 krad/h). Each aging can could be temperature controlled to ±0.3°C from ambient temperature to 150°C. A slow, steady flow (~30 cc/min) of air was supplied to each can throughout the experiment. A detailed description of the aging facility has been published previously. [4]

TENSILE TESTING

Tensile tests were performed using a Model 1000 Instron Table Model Testing Machine equipped with pneumatic grips and having an extensometer clamped to the sample. Samples were strained at ambient temperature at 12.7 cm/min using an initial jaw separation of 5.1 cm. At each aging condition (dose rate, temperature and time), typically 3 or more samples were tested and the data averaged to obtain the results used in the analyses. The unaged elongations for the materials of Table 1 are listed in the Table.

RESULTS AND DISCUSSION

REVIEW OF APPROACH

Dose-Rate Effects

Figure 1 offers a convenient schematic format for discussing aging effects under combined radiation and thermal conditions. The dose to equivalent damage (DED) for some specified degradation property is plotted against the dose rate at a constant temperature, T_1, for both inert and air aging conditions. The DED might represent, for example,

TABLE 1

Material Characteristics

Material Abbreviation	Type	Manufacturer Designation	~Wall Thickness mm	Initial elongation (e_o), %
Hypalon-B	Insulation	Kerite FR cable	1.4	274
Hypalon-C	Inner Jacket	Anaconda Flameguard	0.4	340
Silicone	Insulation	Rockbestos SR cable	1.1	420
ETFE-A*	Insulation	Teledyne Thermatic cable	0.3	173
ETFE-B*	Insulation	unknown-obtained from Savannah River	0.4	305
CLPE	Insulation	General Electric Vulkene Supreme	0.8	345
PVC	Jacket	General Cable Corp.	1.3	310
LDPE	Insulation	General Cable Corp.	0.8	550
Neoprene	Jacket	Okonite	1.5	185
Hypalon-A	Jacket	Kerite FR cable	1.5	300

* ETFE = ethylene-tetrafluoroethylene

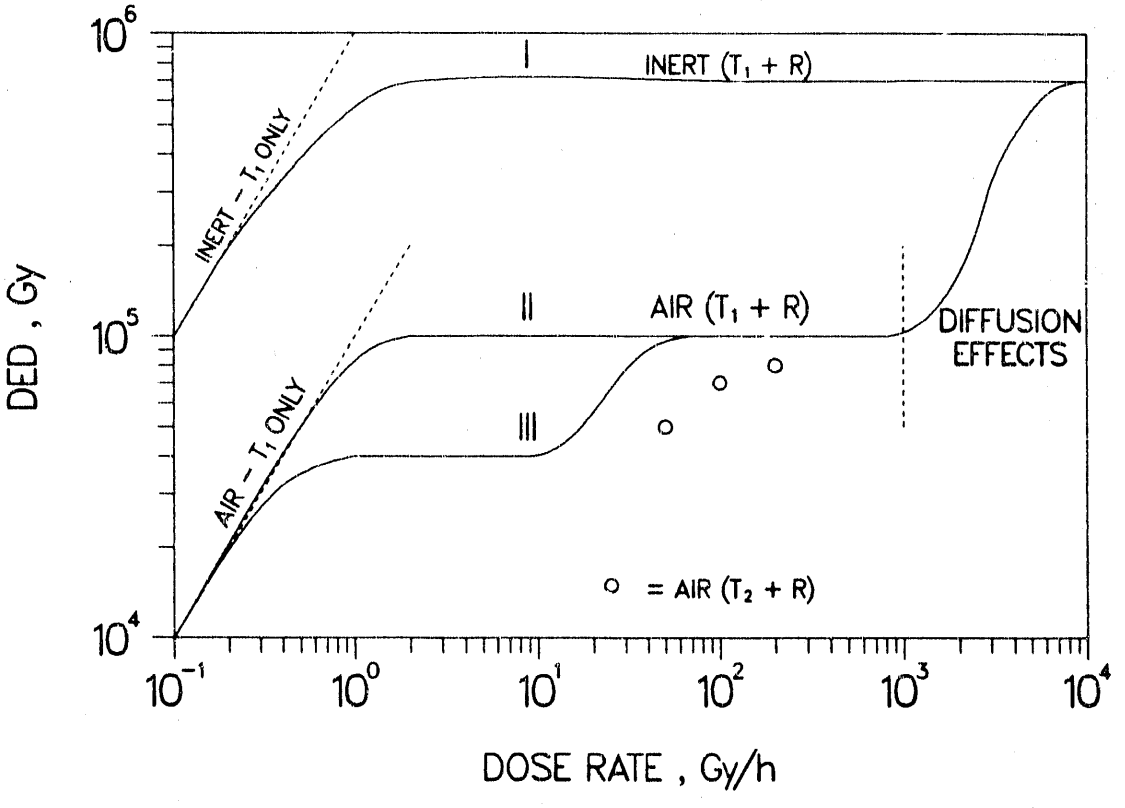

Fig. 1. Schematic illustrating the types of dose-rate effects which can occur in radiation-aged polymeric materials.

the dose required for the ultimate tensile elongation of a material to decrease to 50% of its original (unaged) value. The present figure schematically represents a material where degradation occurs slower in inert environments than in air, a common but not universal situation. For dose-rate regions where neither "chemical" nor "physical" dose-rate effects [3] occur for a given material, the DED would be independent of dose rate and therefore be expressed as a horizontal line. In air environments, diffusion-limited oxidation will become important above a certain dose rate. [3,5-11] For many materials, the resulting reduction in oxidation at the higher dose rates leads to reductions in the degradation rate. In such cases the DED will increase with increasing dose rate, as indicated by the upward curvature of curve II toward the right hand side of the figure. Eventually, at high enough dose rates, oxidation will be confined to a small region near the sample surfaces. This small amount of oxidation can often be insignificant compared to the inert aging of the bulk of the sample. The DED will then approach the inert aging line as indicated. The dividing line between homogeneous oxidation and heterogeneous diffusion-limited oxidation, which is indicated schematically in the figure, can be estimated using the techniques discussed [3] in the previous report- i.e., by using theoretical expressions [9] or by direct profiling experiments on the aged samples. [6-10] Separating the homogeneous aging data from potentially-anomalous heterogeneous results is the first important requirement before attempting to model and then extrapolate accelerated laboratory data to long-term ambient aging conditions.

Deviations from the horizontal behavior shown for lines I and II must also occur on the low-dose-rate side of the figure because the dose rates eventually become small enough such that thermal aging effects alone will dominate the deterioration. In this low dose-rate limit, the time for a certain amount of degradation will be a constant determined solely by the time required for thermal degradation at T_1, the temperature of interest. In terms of the log-log format used in Fig. 1, the constant time condition appropriate to the thermal-only limit will be represented by a straight line (iso-chrone) with slope equal to unity. As an example, if thermal aging in air at T_1 causes the degradation parameter of interest to reach its appropriate value (e.g., 50% of initial elongation) after 1×10^5 h, then the thermal aging limit line (at a temperature of T_1) is as shown in Fig. 1. Whereas dose-rate independence (horizontal behavior) may be valid for air aging (e.g., line II) at the intermediate dose rates shown in Fig. 1, it is clear that the results at lower dose rates must asymptotically approach the thermal-only line. Similar arguments hold for the inert aging case (line I) at low dose rates. Although it appears to be a dose-rate effect when plotted as in Fig. 1, it might be argued that this asymptotic approach at low dose rates to the thermal only line does not always represent a true "chemical" dose rate effect. This argument would be justified, for instance, if there were no interactions between the thermal and radiation degradation pathways (e.g., they simply act in parallel). On the other hand, when interactions do exist, this low dose rate dropoff will represent a true "chemical" dose-rate effect.

For air environments, there are other types of chemical dose-rate effects. These will occur whenever an important rate-limiting step in the oxidation chemistry occurs on a timescale similar to the experimental timescale. The result will be a third class of dose-rate effects (i.e., regions of non-horizontal behavior), yielding situations represented schematically by the intermediate dropoff region of curve III in the figure. One example is the slow reactions of long-lived radicals, such as those trapped in the crystalline regions of partially crystalline polymers. Other examples include the rate-determining breakdown of intermediate hydroperoxide species, described in the earlier report [3] and the related copper-catalyzed oxidation effects. [12] For the PVC jacket material discussed in the earlier report, [3] the hydroperoxide mechanism resulted in a curve which resembles the intermediate to high dose-rate portions of curve III.

For the purposes of discussing accelerated aging, we now consider the effect of raising the temperature of the radiation experiments in air above T_1. In general raising the exposure temperature at a given dose rate will hasten the degradation. Hypothetical data at 50, 100 and 200 Gy/h and a temperature T_2 ($>T_1$) are plotted as the three circles in Fig. 1. Clearly the asymptotic, thermal-only isochrone at T_2 will be shifted to the right from the T_1 line by the thermo-oxidative acceleration factor appropriate to this temperature difference. The goal of extrapolated predictions is to take accelerated radiation-aging data at various dose rates and temperatures (e.g., T_1, T_2, etc.) and utilize these data to generate predictions at the use temperature under much lower dose rate conditions. From Fig. 1, this will first entail separating out the potentially anomalous heterogeneously-oxidized results, followed by appropriate modelling of the remaining homogeneously oxidized data.

Time-Temperature Superposition

We will review below our approach for extrapolating accelerated, short-term combined radiation-thermal aging experiments to longer times at much lower dose rates. This approach, which we refer to as time-temperature-dose rate superposition, is based on generalizing the well-known time-temperature superposition procedure used in thermal aging situations. A brief review of the salient features of time-temperature superposition will be helpful for understanding the more complex combined-environment modelling. Thermal aging studies are often conducted such that isothermal, time-dependent degradation data at a number of temperatures are generated. An example is illustrated in Fig. 2, where changes in the ultimate tensile elongation are plotted versus log of the time for the air aging of a commercial chloroprene cable jacketing material. Time-temperature superposition assumes that raising the temperature by a certain amount from T_1 to T_2 increases the degradation rate by a constant multiplicative factor a_{12} which is independent of the degradation level. This corresponds to having constant shapes for isothermal degradation data when plotted versus log time, as is clearly the case for the chloroprene data. When constant

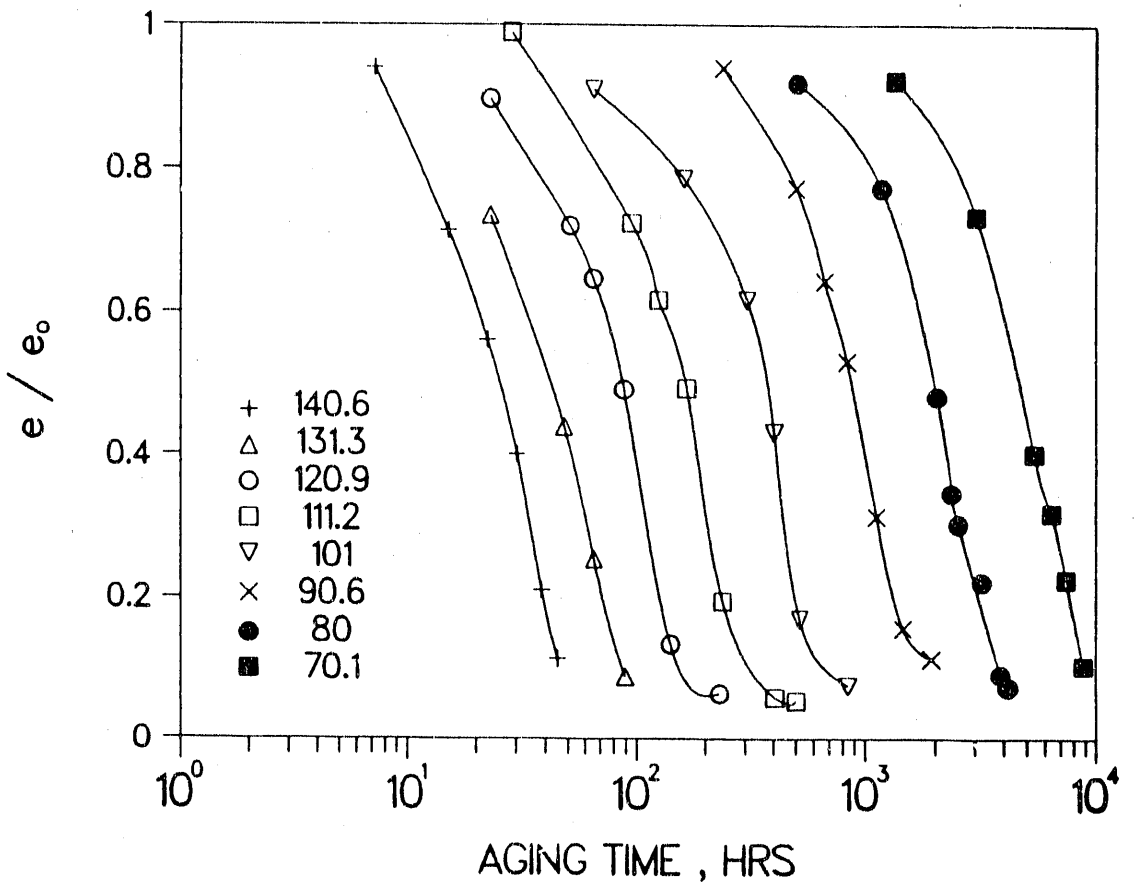

Fig. 2. Ultimate tensile elongation of aged materials divided by the unaged value (e/e_o) versus aging time in air under the indicated isothermal aging conditions for a neoprene cable jacketing material.

acceleration occurs, the next step is to determine the relationship between the empirical multiplicative factors and the temperatures. When the degradation is caused by chemical reactions occurring within the organic material, the Arrhenius relationship

$$a_{ij} = \exp \frac{E_a}{R} [T_i^{-1} - T_j^{-1}] \qquad (1)$$

is often observed, where E_a is the effective activation energy for the degradation process and R is the gas constant. This relationship implies that a plot of log (time) to an equivalent amount of damage versus the inverse temperature (in $°K^{-1}$) will be linear, and that the slope of the line equals E_a. For well-behaved materials, the same Arrhenius relationship holds regardless of the amount of degradation, implying that the chemistry does not change radically with degradation level. An Arrhenius plot of the data of Fig. 2 gives E_a = 21 kcal/mol, which we now use to shift all the data to a common temperature, selected to be 45°C. The results, shown in Fig. 3, indicate that excellent time-temperature superposition exists over a large temperature range (70°C to 140°C). Coupled with the easily-rationalized Arrhenius form for the relationship between time and temperature, this gives us reasonable confidence in extrapolating these data to lower temperatures, thereby allowing predictions at longer, experimentally inaccessible times. We have already done this in Fig. 3 by shifting to 45°C, yielding predictions for times approaching 20 years at this temperature.

Although time-temperature superposition has been successfully applied to polymers for many years, it is sometimes found to be inappropriate. For one thing, the complicated chemistry underlying the changes in the degradation parameter may result in a non-Arrhenius temperature dependence due to competition between processes of differing activation energies. Likewise, superposition should not in general be expected when a physical transition of the polymer, such as the glass transition or crystalline melting temperature, occurs within the temperature range of the accelerated experiments or the temperature range of the extrapolation. Whenever thermal aging data cannot be superposed, extrapolations can be difficult and inaccurate. Even when superposition occurs and a simple relationship (e.g., Arrhenius) between time and temperature exists, the empirical nature of time-temperature superposition must be remembered. Very seldom does enough knowledge exist of the complex kinetics underlying the degradation such that an empirical activation energy can be unambiguously derived.

Time-Temperature-Dose Rate Superposition [3]

Time-temperature-dose rate superposition represents an extension of the empirical time-temperature superposition approach to combined radiation plus thermal environments. Hypothetical dose to equivalent damage (DED) versus dose rate results, given in Fig. 4, are useful for understanding the procedures involved in this approach. The three curves passing through the points labelled c_i, b_i and a_i, respectively, where i = 0,1,2, represent combined radiation plus thermal data at the

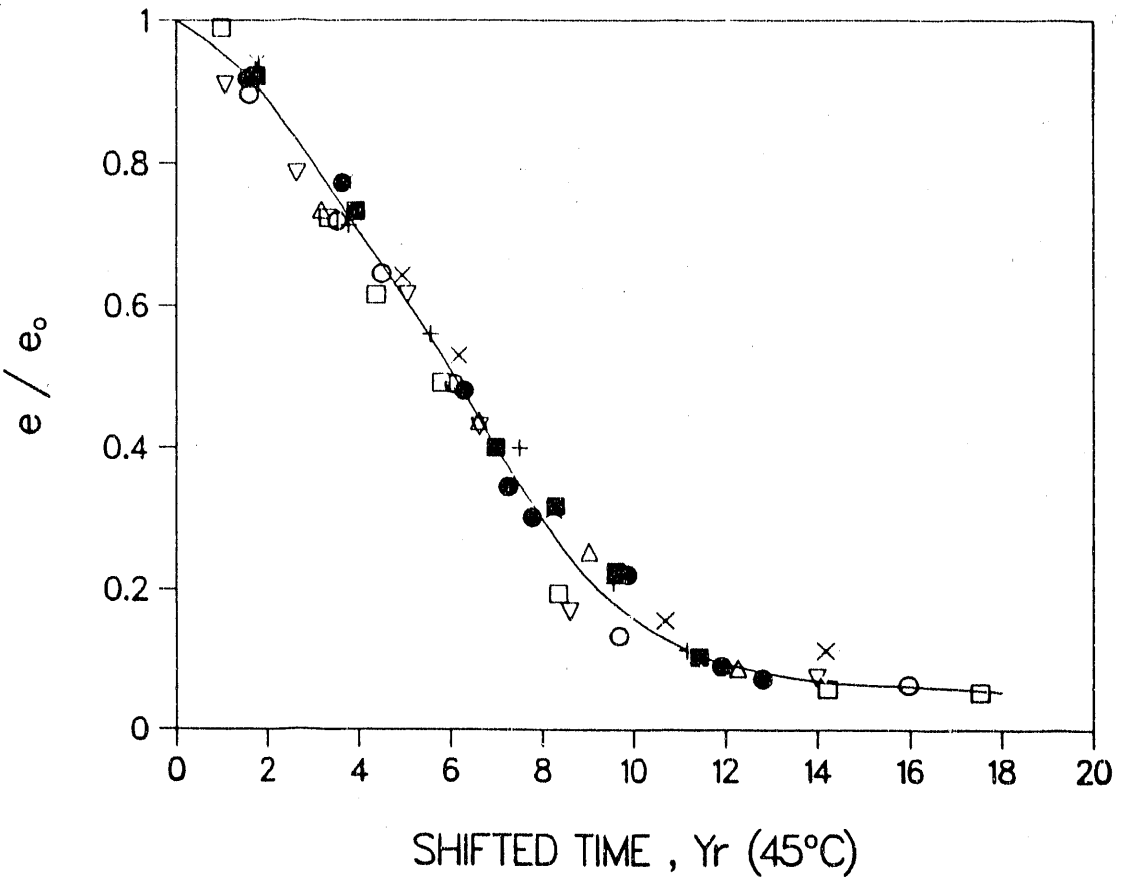

Fig. 3. Time-temperature superposition at 45°C of the neoprene thermal-only aging data of Fig. 2. An Arrhenius activation energy of 21 kcal/mol was utilized to shift the results.

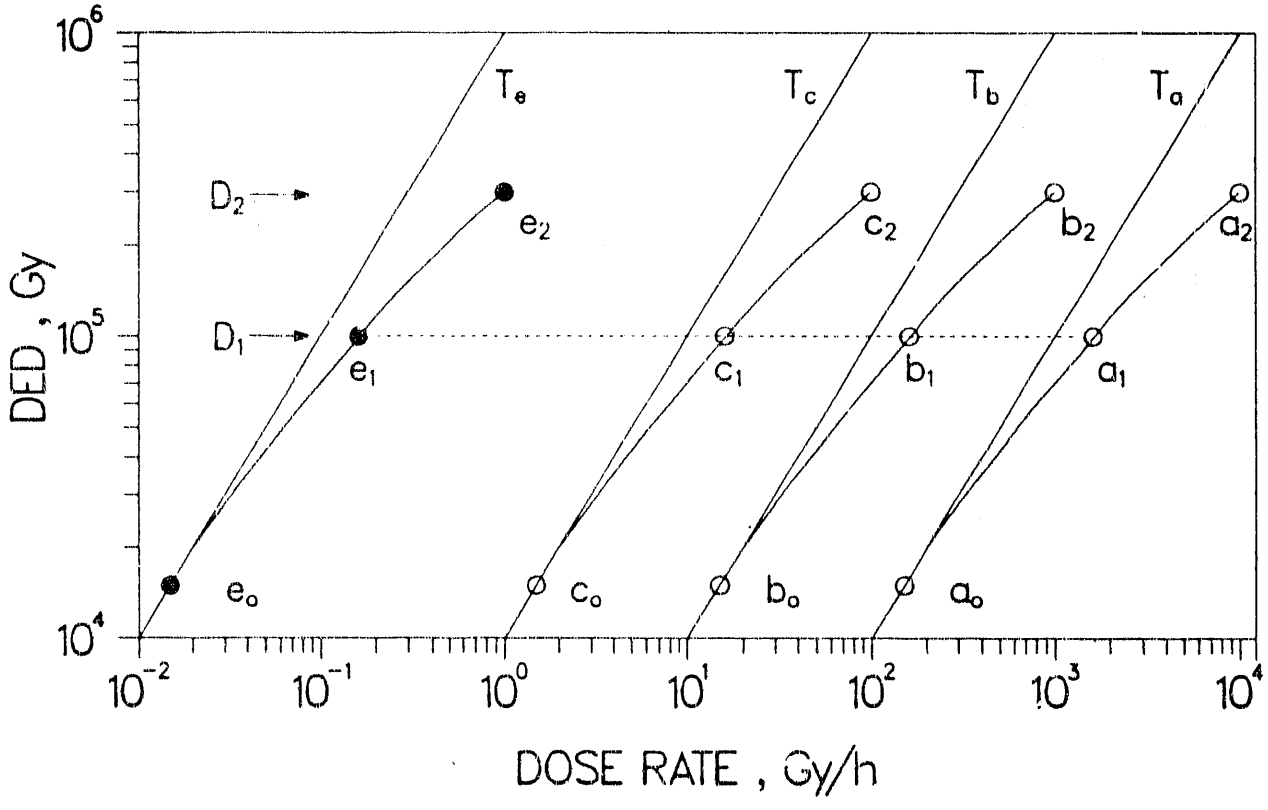

Fig. 4. Hypothetical dose to equivalent damage (DED) results versus dose rate, under several isothermal conditions.

three temperatures T_c, T_b and T_a. The straight lines of unit slope (isochrones), labelled T_c, T_b and T_a represent the times to equivalent damage at these temperatures in the absence of radiation. Therefore, at low enough dose rates, the combined-environment curves must approach these thermal-only limits, as indicated at a_o, b_o and c_o. We now turn our attention to the dashed "isodose" line at a DED value of D_1 and its intersection with the three isothermal combined-environment curves at the points labelled c_1, b_1 and a_1. These points give combinations of temperature and dose rate conditions which yield equivalent degradation after precisely the same total dose, D_1. Since the time to a constant total dose is inversely proportional to the dose rate, these points have the interesting property that, for a given pair, the ratio of the times appropriate to their respective temperatures is exactly equal to the inverse of the ratio of their respective dose rates. In other words, if we empirically determine the functional relationship between time and temperature for combined radiation plus thermal environments under isodose conditions, the same relationship exists between inverse dose rate and temperature. Analogous to time-temperature superposition, once this isodose relationship between time and temperature is determined, it can be extrapolated to a lower temperature under the same isodose condition. This extrapolation to a temperature T_e is shown conceptually by the point e_1 in Fig. 4. Point e_1 would then represent the superposition of data points a_1, b_1 and c_1 after each point has been horizontally shifted to the temperature T_e by its appropriate shift factor. By finding the functional relationship between data such as a_2, b_2 and c_2 at another isodose level (e.g., D_2) and extrapolating this relationship, another predicted point (e_2) can be generated. In the most general case, the empirical functional relationships between time and temperature would be complex, dependent on isodose level and dependent on the particular value of DED chosen for analysis. Trying to extrapolate results in such a situation would require extreme caution, analogous to attempting an extrapolation of a non-Arrhenius, damage-level-dependent relationship derived from thermal-only aging experiments. The best situation for confident extrapolations would involve a simple, easily-rationalized relationship which was independent of both the isodose value at a particular damage level and the damage level itself. Although not strictly necessary for applying the above empirical superposition approach, we will restrict ourselves to such simplifications for the discussion that follows. In particular, since it is the easiest relationship to rationalize, we will only allow Arrhenius relationships between time and temperature. In other words, we will attempt to superpose data by assuming that an Arrhenius expression relates time and temperature under isodose conditions and that the appropriate value of E_a is independent of both the isodose level and the damage level selected.

Since it is impossible to know beforehand the particular sets of combined radiation plus temperature conditions which yield isodose data, Fig. 4 represents an idealized situation. The two right hand curves in Fig. 5 show how real data might appear. The three circles on the curve labelled 80 might represent data taken at 80°C and three different dose rates whereas data at 100°C and three dose rates might be represented by

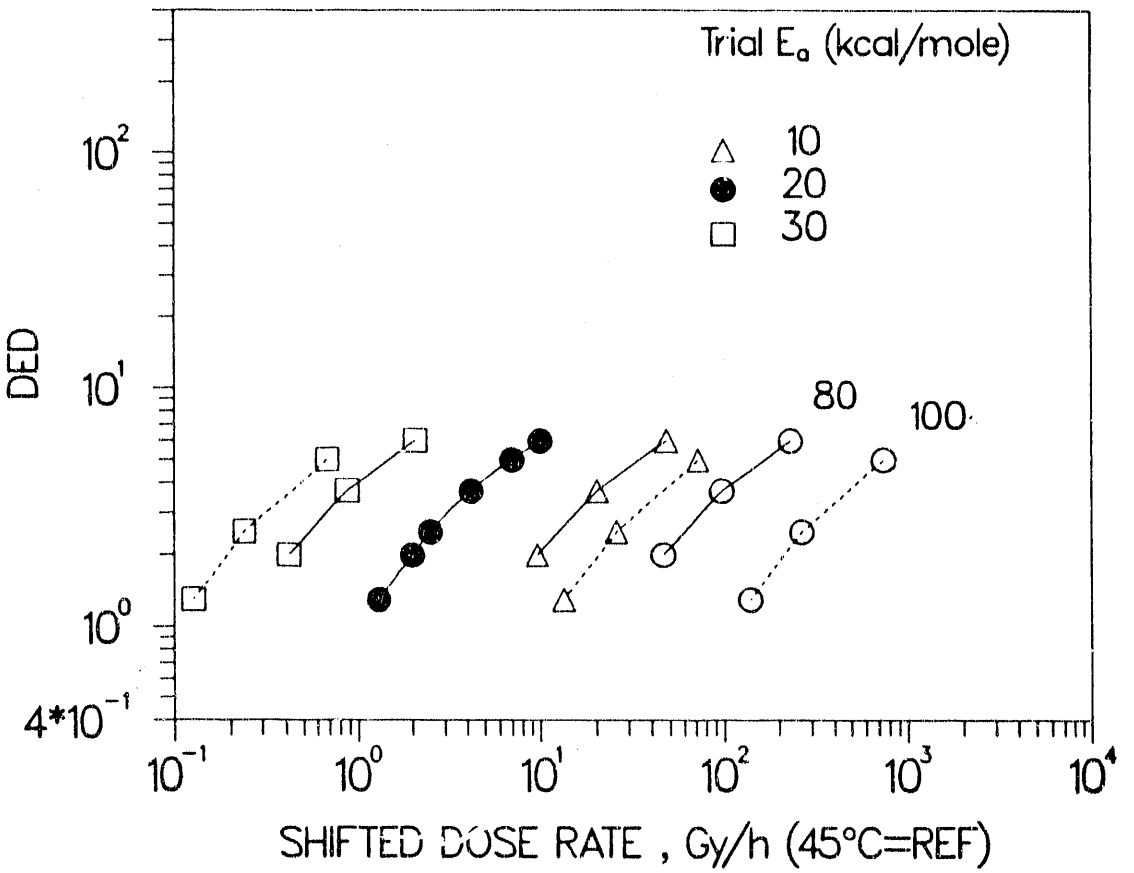

Fig. 5. Hypothetical dose to equivalent damage (DED) results at two temperatures (80°C and 100°C), plus shifted results for three trial values of the shifting activation energy, E_a. This illustrates the procedures involved in empirically determining the value of E_a which yields the best time-temperature-dose rate superposition.

the points on the curve labelled 100. Since we are currently restricting ourselves to a single value of the Arrhenius activation energy, the time-temperature-dose rate superposition procedure involves horizontally shifting the six data points at 80°C and 100°C using various trial values of E_a until reasonable superposition results. In the present example, we have shifted the data to a 45°C reference temperature using three trial values for E_a (10, 20 and 30 kcal/mol). From eq. (1) above, the 80°C data shift, for example, by a factor in time (or, equivalently, in inverse dose rate) of 23.1 when E_a = 20 kcal/mol. Superposition occurs for an activation energy of 20 kcal/mol; for lower values of E_a, the 100°C data are not shifted enough to coalesce with the shifted 80°C data; for higher values of E_a, they have shifted beyond the 80°C data.

Since our procedure empirically determines E_a by looking for the best overall superposition of combined-environment data, any value of E_a is theoretically possible. However, if the data encompass conditions where important thermal-only contributions are expected, then our simplifying restriction that E_a be independent of isodose level forces E_a to equal the activation energy for thermal degradation in the absence of radiation. This is obvious from Fig. 4, where the time-temperature relationship between the thermal-only dominated points a_o, b_o and c_o is the thermal-only Arrhenius relationship. If, however, the combined-environment conditions are far away from the region where thermal-only effects are important, some other value of E_a is possible. Examples of both cases were described in our earlier report. [3]

Assuming equivalent data scatter, it should be noted that the uncertainties in the derived values of the activation energies using time-temperature-dose rate superposition are usually higher than those derived from time-temperature superposition of thermal-only data. The uncertainty in E_a for the combined-environment method will increase as the dose-rate effect decreases. This is obvious from examining the hypothetical data of Fig. 5. If the dose-rate effect for the shifted data approaches a slope of one (e.g., equivalent to thermal-only), the uncertainty in E_a for time-temperature-dose rate superposition will approach the uncertainty in E_a for time-temperature superposition of thermal-only results. At the other extreme, if the data at 80°C and 100°C were horizontal at the same DED value, superposition would be possible for any value of E_a (e.g., "infinite" uncertainty). Large uncertainties in E_a can also result when small to moderate dose-rate effects are coupled with large amounts of scatter in the raw data.

Again we must caution that time-temperature-dose rate superposition may not always be appropriate for cases where accelerated data are taken, or extrapolation attempted, across a thermal transition of a polymer. This potential complication will be discussed in detail in a forthcoming report, where we will examine results for crosslinked polyolefin (CLPO) and EPDM cable insulation materials, two of the most widely-used generic materials in existing United States nuclear power plants.

APPLICATION OF METHODOLOGY TO CABLE MATERIALS

Hypalon-B Insulation

The hypalon-B insulation material was aged in a series of combined radiation-thermal exposures under continuous air-flow conditions. Dose rates and temperatures ranged from approximately 10 Gy/h to 2 kGy/h and from ambient to 140°C, respectively. Under each of the experimental conditions, ultimate tensile elongation data were obtained versus aging time and the data used to estimate the dose required for the elongation to drop to various levels from its initial value (e_o) of 274%. Figure 6 gives the dose required for e/e_o to reach 0.6 (e.g., for the absolute elongation to reach 204%) versus the dose rate and temperature (numbers by the data points in °C) of the combined-environment experiments. Since the results imply that either raising the temperature or lowering the dose rate tends to increase the degradation rate per unit dose, dose-rate effects are clearly present. Some of the data points come from relatively long-term exposures; for instance, the result at ~12 Gy/h plus 22°C represents an almost seven year exposure.

As pointed out in the earlier publication, [3] before these data can be analyzed using the time-temperature-dose rate shifting methodology, we must eliminate from the analysis any data points which are taken on samples aged under diffusion-limited oxidation conditions. This can be done by determining the samples which are heterogeneously oxidized either by direct experimental profiling techniques [6-10] or through the use of theoretical expressions. In particular, if measurements exist or estimates can be made for the oxygen consumption rate (Φ) and the oxygen permeation rate (P_{ox}) for a material of thickness L, surrounded on both sides by oxygen of partial pressure p, significant diffusion effects will occur whenever [9]

$$L^2 \Phi/(P_{ox}p) > 8 \qquad (2)$$

Seguchi and co-workers [13,14] obtained values for P_{ox} and Φ on a commercial hypalon material. Their results allow us to estimate that only one of the experiments in Fig. 6 was conducted under diffusion-limited oxidation conditions; [3] this point is plotted using a triangle. The remaining data points (plotted as circles) represent homogeneously oxidized materials; these are the data points which can be safely analyzed using the time-temperature-dose rate superposition methodology.

When the approach outlined in Fig. 5 is used to analyze these data points, we find that reasonable superposition occurs for an E_a = 18±4 kcal/mol. It turns out that thermal-only aging data give good superposition using an E_a = 21±2 kcal/mol, as seen by the time-temperature superposed results given in Fig. 7 at a reference temperature of 45°C. Since the combined dose rate/thermal conditions were conducted in regions where thermal-only effects are important over the time scales probed, and since the two activation energies agree

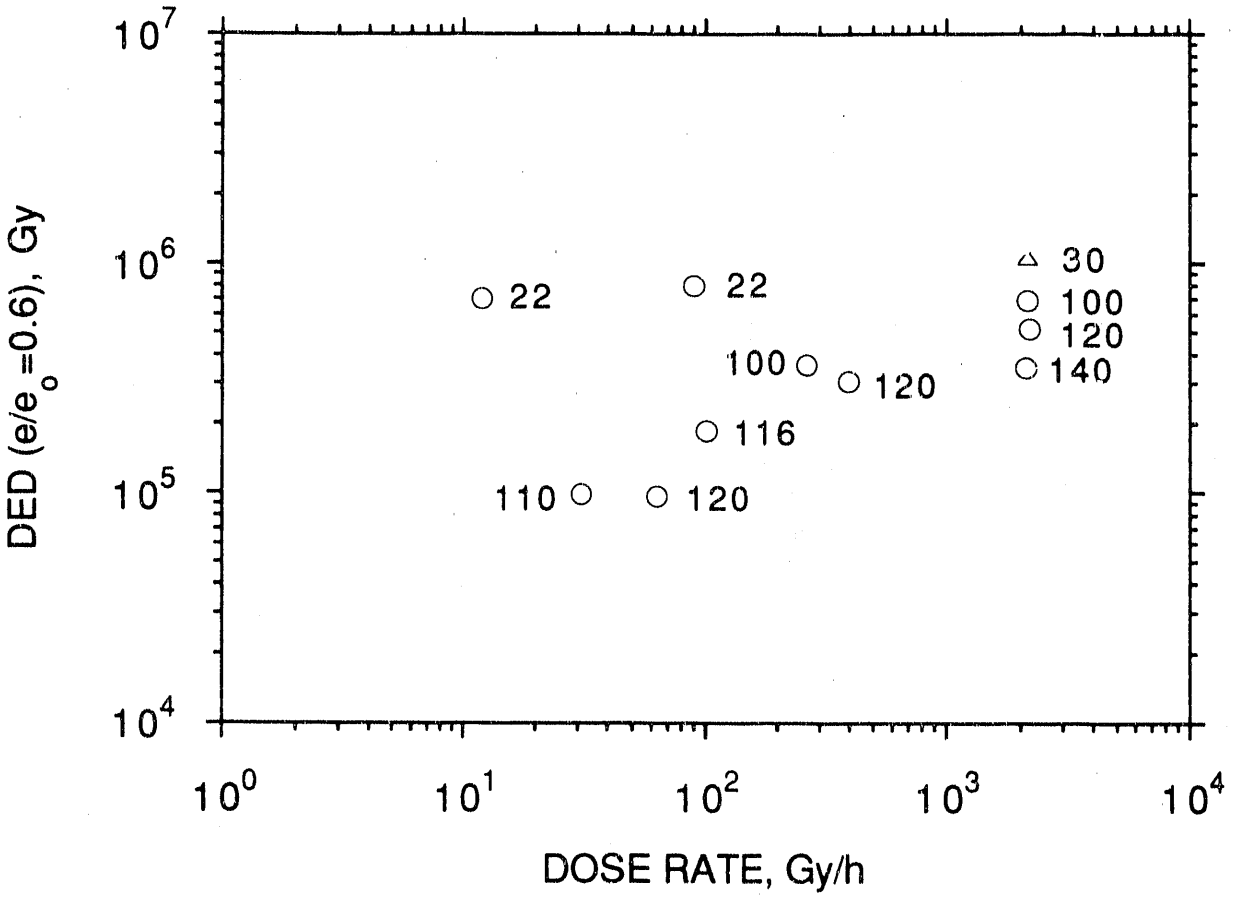

Fig. 6. Radiation dose required for the ultimate tensile elongation of hypalon-B to decrease to 60% of its unaged value at various combinations of dose rate and temperature (the numbers by the data points give the temperature in °C). Aging conditions that likely result in homogeneously oxidized materials are plotted as circles; the data point plotted as a triangle represents aging conditions where important diffusion-limited oxidation effects are suspected.

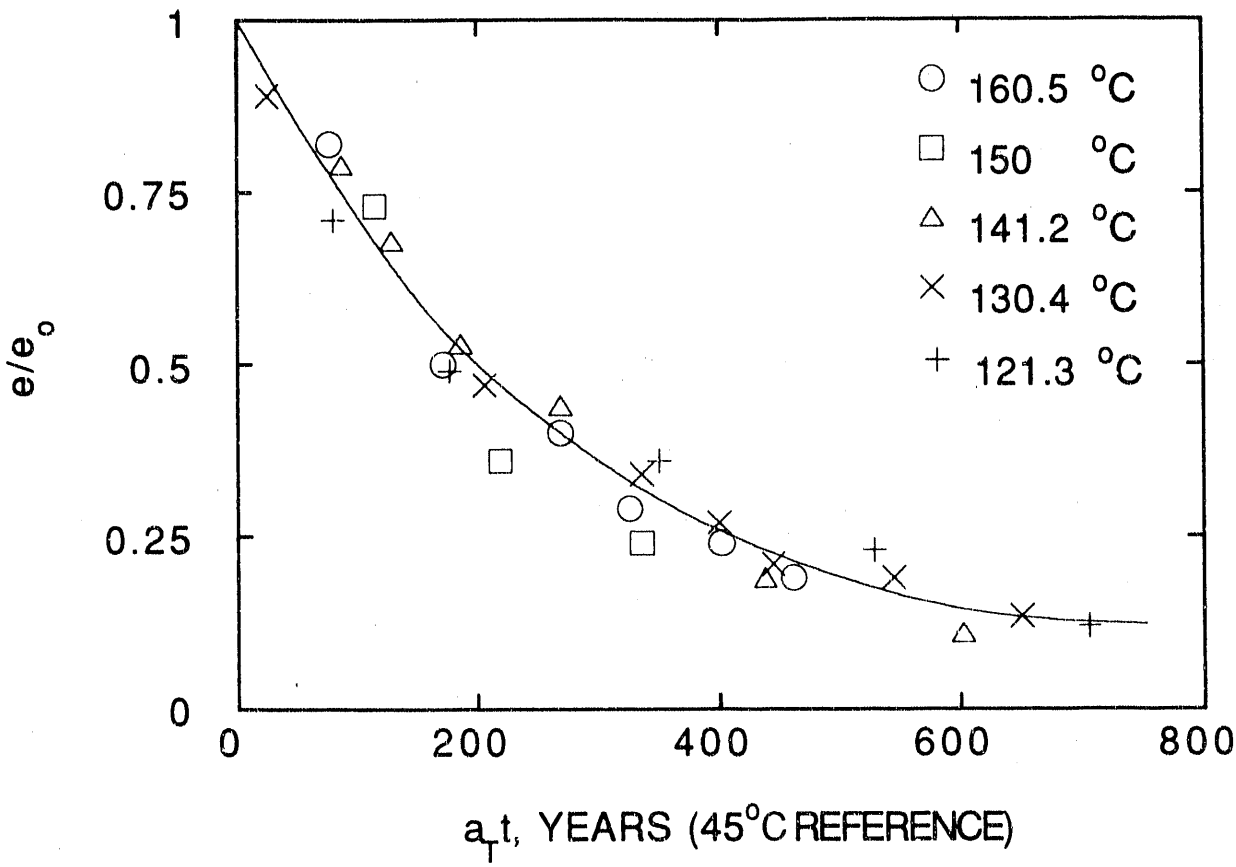

Fig. 7. Time-temperature superposed results at a reference temperature of 45°C for thermal-only aging results on the hypalon-B insulation material. An activation energy of 21 kcal/mol was used for the shifting.

within the experimental uncertainties, we will use the more accurately determined thermal activation energy to shift the combined-environment data. The bottom curve through the open circles in Fig. 8 shows the resulting time-temperature-dose rate superposed predictions for e/e_o = 0.6 (204%) at 45°C. Good superposition is evident and the use of the thermal activation energy for shifting the combined-environment data results in the easily rationalized, asymptotic approach of the low dose rate data towards the thermal-only limit (lower isochrone). Further confidence in the superposed results comes from the observation that the long-term (~seven year) point (second point from the right) lies on the superposed predicted curve.

Also shown in Fig. 8 (filled circles) are the shifted results for a higher level of degradation, corresponding to the dose required for the elongation to drop to 100% absolute. It is clear that the use of a 21 kcal/mole activation energy leads to excellent superposition for this hypalon material, regardless of the level of degradation chosen. Whenever the superposition is independent of the amount of degradation, enhanced confidence in the methodology predictions will clearly result.

The superposed curves now allow predictions to be made under very low dose rate conditions, similar to those that might occur during nuclear power plant ambient aging. At 0.1 Gy/h (10 rad/h) plus 45°C, for instance, the top curve predicts that the elongation of this hypalon insulation will drop to 100% absolute after ~230 years. Results at different dose rates and temperatures can be readily generated. For example, predictions versus dose rate at 30°C are obtained by a simple horizontal shift of the 45°C curves to the left by a factor of 5.18, calculated using eq. (1).

Hypalon-C Jacket

Tensile property results were obtained versus aging time for the thin hypalon jacket material (hypalon-C) under a very limited number of combined-environment conditions. Data representing the dose required for the elongation to drop to 60% of its initial value (e_o = 340%) are plotted versus dose rate and temperature in Fig. 9. As is often observed, dose-rate effects are indicated since either raising the temperature at constant dose rate or lowering the dose rate at constant temperature tends to increase the degradation rate per unit dose. In addition to the combined-environment experiments, thermal-only exposures were conducted versus time at 5 temperatures ranging from 100°C to 150°C. Reasonable time-temperature superposition of the thermal-only elongation data is possible using an activation energy of 25 kcal/mole, as shown in Fig. 10 at a reference temperature of 45°C. When this activation energy is used to shift the combined-environment results of Fig. 9 and similar combined-environment results at e = 100% absolute, reasonable time-temperature-dose rate superposition occurs, as seen in Fig. 11. As found for the hypalon insulation above (hypalon-B) and for the hypalon jacket studied in the earlier publication (hypalon-A), the predicted combined-environment curves tend to asymptotically approach the thermal-only isochrones at low dose rates. [3]

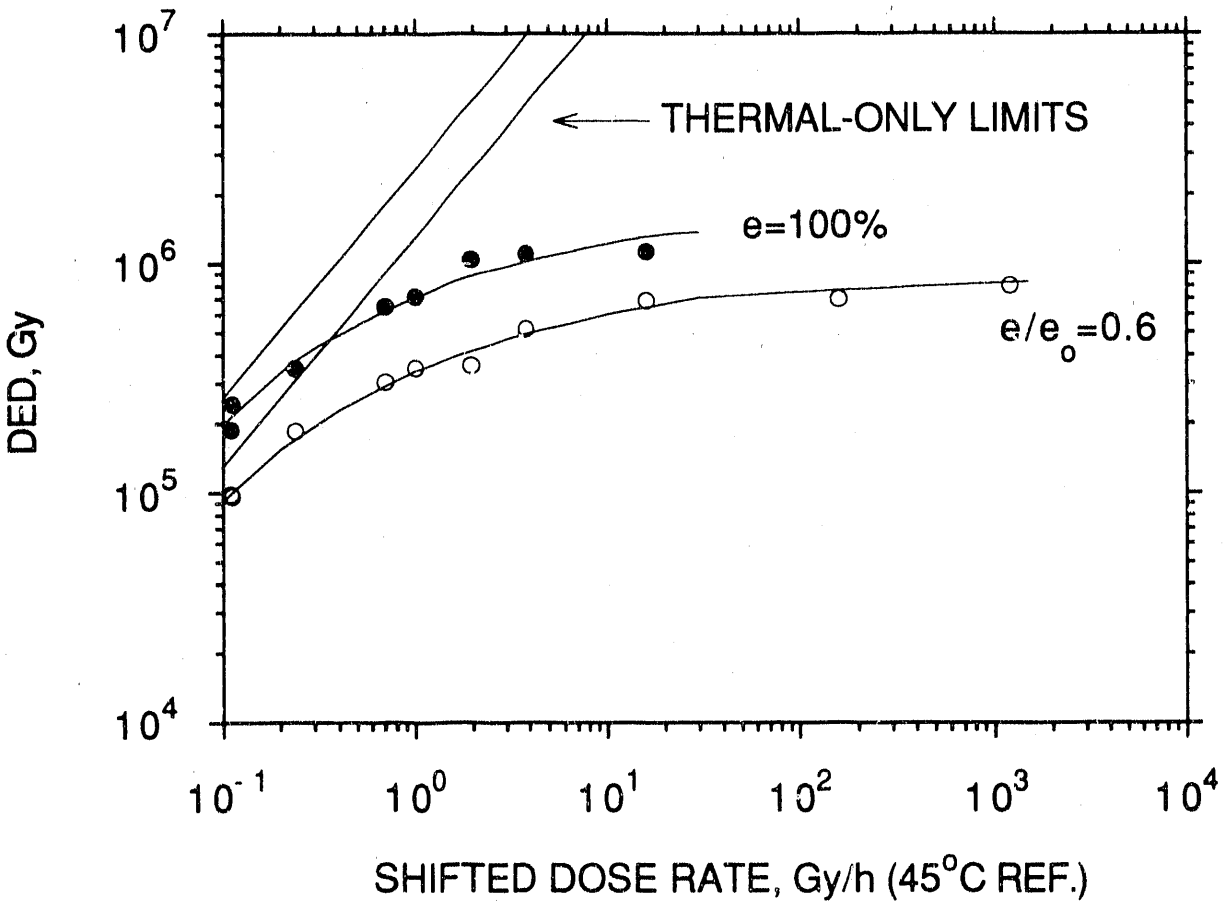

Fig. 8. Predictions for the hypalon-B material of the dose required for the ultimate tensile elongation to drop to 60% of its initial value (open circles) and to 100% absolute (closed circles) versus dose rate at 45°C. The homogeneously oxidized data points of Fig. 6 and similar results at 100% absolute elongation were time-temperature-dose rate shifted according to the methodology using a 21 kcal/mol activation energy. The straight lines of unit slope come from the thermal-only superposed predictions shown in Fig. 7.

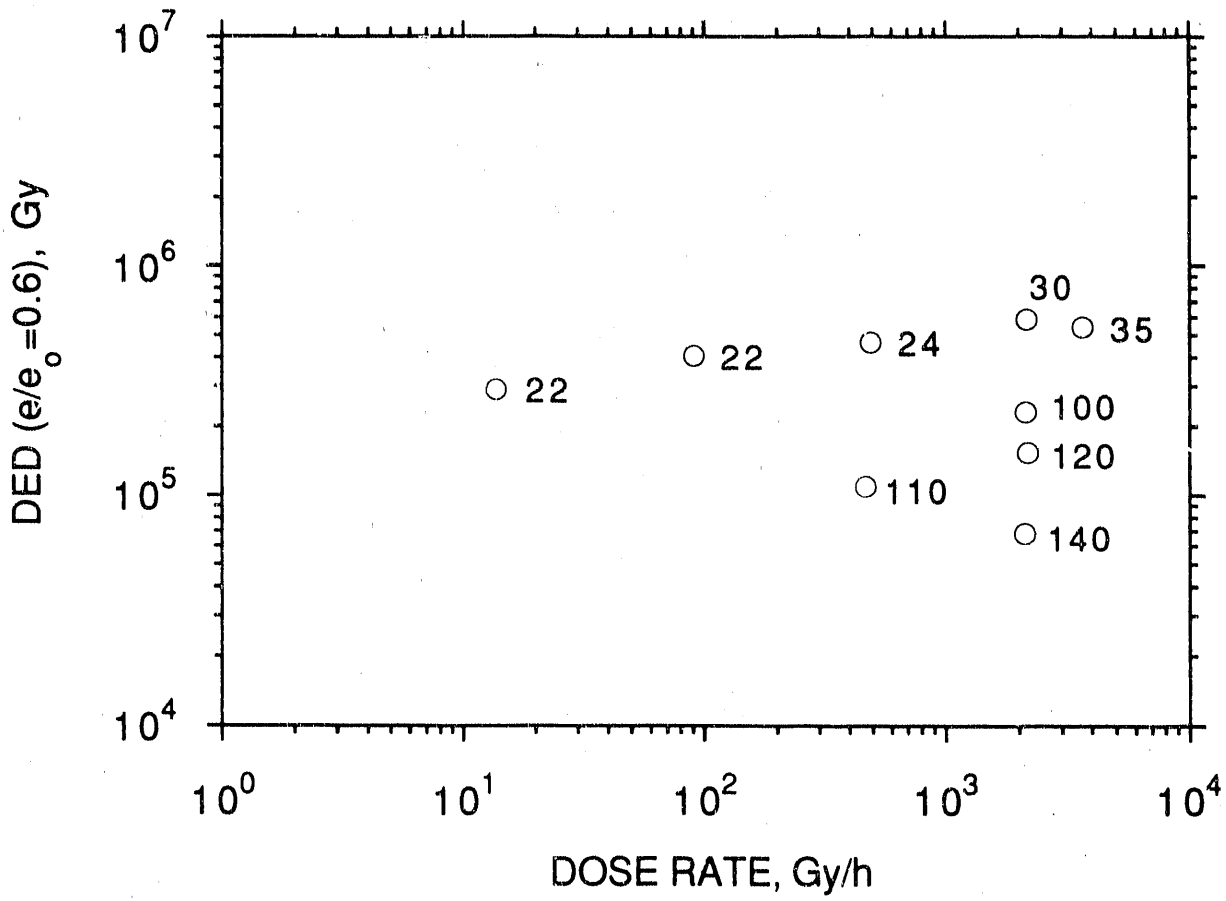

Fig. 9. Radiation dose required for the ultimate tensile elongation of hypalon-C to decrease to 60% of its unaged value at various combinations of dose rate and temperature (the numbers by the data points give the temperature in °C).

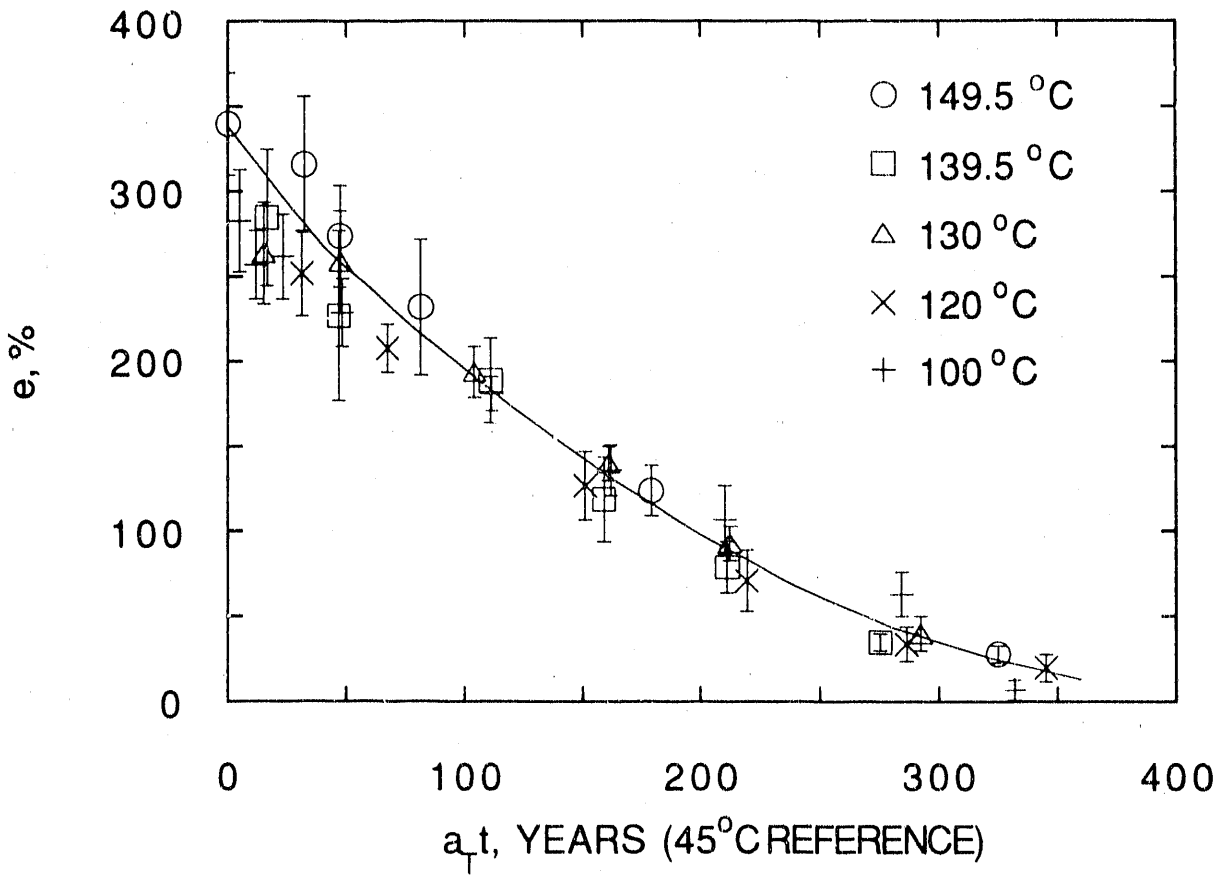

Fig. 10. Time-temperature superposed results at a reference temperature of 45°C for thermal-only aging data on the hypalon-C insulation material. An activation energy of 25 kcal/mol was used for the shifting.

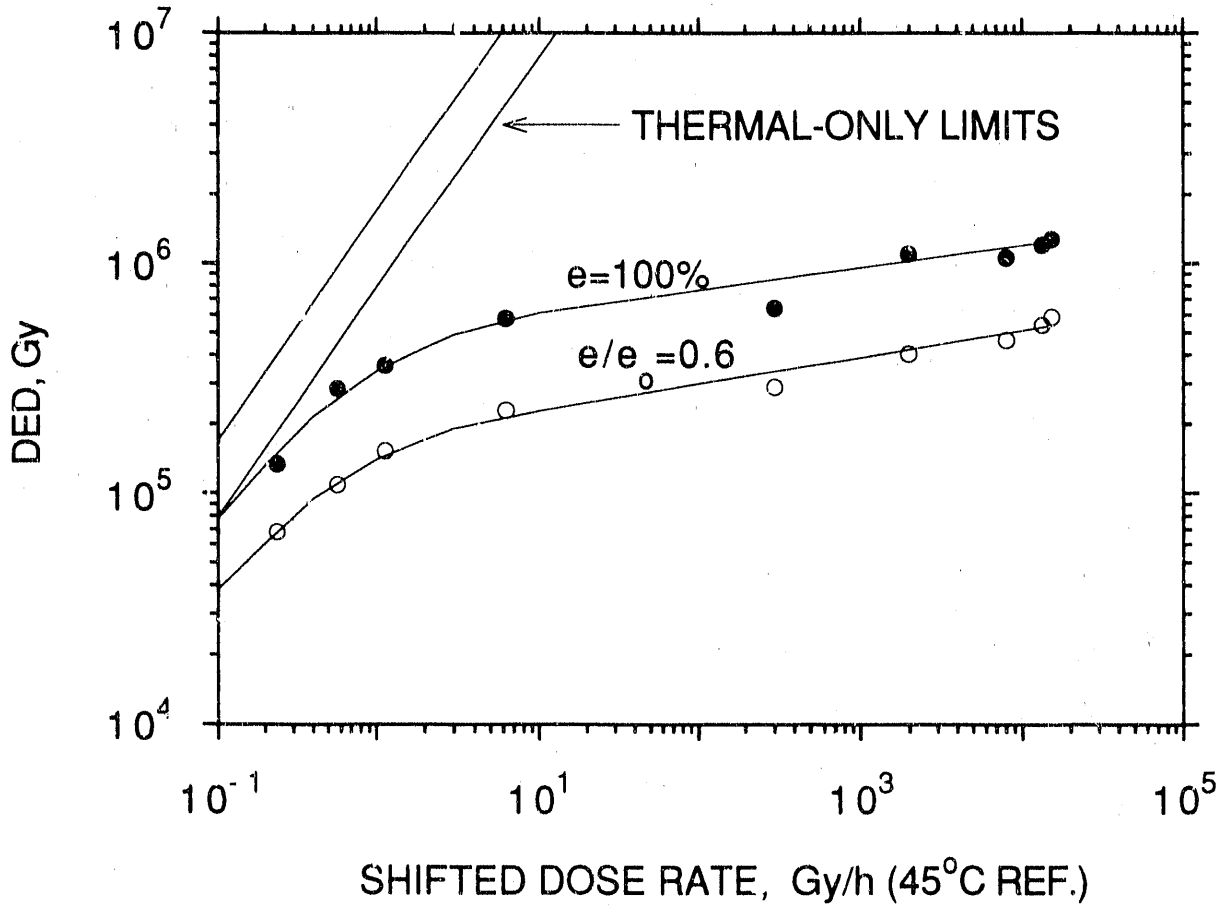

Fig. 11. Predictions for the hypalon-C material, of the dose required for the ultimate tensile elongation to drop to 60% of its initial value (open circles) and to 100% absolute (closed circles) versus dose rate at 45°C. The data points of Fig. 9 and similar results at 100% absolute elongation were time-temperature-dose rate shifted according to the methodology using a 25 kcal/mol activation energy. The straight lines of unit slope come from the thermal-only superposed predictions shown in Fig. 10.

ETFE Insulations

Results on the ETFE materials offer a dramatic example of the potential differences illustrated schematically in Fig. 1 between aging in inert environments and aging in oxygen. Figure 12 shows, for example, a comparison of high dose rate elongation results at 70°C in vacuum versus air for ETFE-A; the data show that degradation occurs at least 5 to 10 times faster in the presence of oxygen. This implies that large physical dose-rate effects caused by the oxygen diffusion-limited mechanism might be anticipated when diffusion limitations are operative. Limited combined-environment results for the two ETFE materials are consistent with this expectation. Figures 13 (ETFE-A) and 14 (ETFE-B) plot the dose required to lower the elongation to 100% absolute versus dose rate and temperature. Triangles are used to denote experimental conditions expected to be influenced by diffusion-limited oxidation effects. [6] The vacuum result obtained from from Fig. 12 is denoted by a V in Fig. 13. It is interesting to note that many nuclear power plant aging simulations are carried out at dose rates above 1000 Gy/h and at ambient temperatures. Since such conditions for ETFE normally guarantee the presence of diffusion-limited artifacts and therefore reduced degradation rates, these simulations may significantly urderestimate material damage caused by radiation aging.

Once the diffusion-limited points are eliminated, it is clear that the homogeneously oxidized samples show little dependence on either dose rate or temperature. This makes it difficult to apply the time-temperature-dose rate superposition methodology since any activation energy will lead to superposition of horizontal data. This situation can occur whenever insufficient data exist or the data available show only minor dose-rate effects. In such instances, it is still possible to make predictions by assuming a reasonable activation energy is appropriate to the shifting. For ETFE in thermal (air) aging environments, a 21 kcal/mol activation energy is found to result in excellent time-temperature superposition. [15] In our previous report, [3] good time-temperature-dose rate superposition was found for activation energies of 21 kcal/mol (neoprene jacket), 24 kcal/mol (hypalon-A jacket), 23 kcal/mol (PVC jacket) and 16 kcal/mol (low density polyethylene insulation); in this report, 21 and 25 kcal/mol gave reasonable results for the hypalon-B insulation and the hypalon-C jacket material, respectively. With the above in mind, we use 21 kcal/mol to shift the homogeneously-oxidized data of Figs. 13 and 14 to a 45°C reference temperature; the results are plotted as open (ETFE-A) and closed (ETFE-B) circles in Fig. 15. Thus, for the two ETFE materials studied, we conclude that aging under radiation conditions which result in homogeneous oxidation will reduce the elongation to ~100% after $9\pm3 \times 10^4$ Gy, independent of dose rate and temperature. Since few additives beyond coloring agents are used for ETFE materials, we would expect that other ETFE materials might behave similarly.

Although we carried out our analyses at 100% absolute elongation, the results for air-aged ETFE materials show only minor dependence on the damage criterion selected. This is due to the observation that once

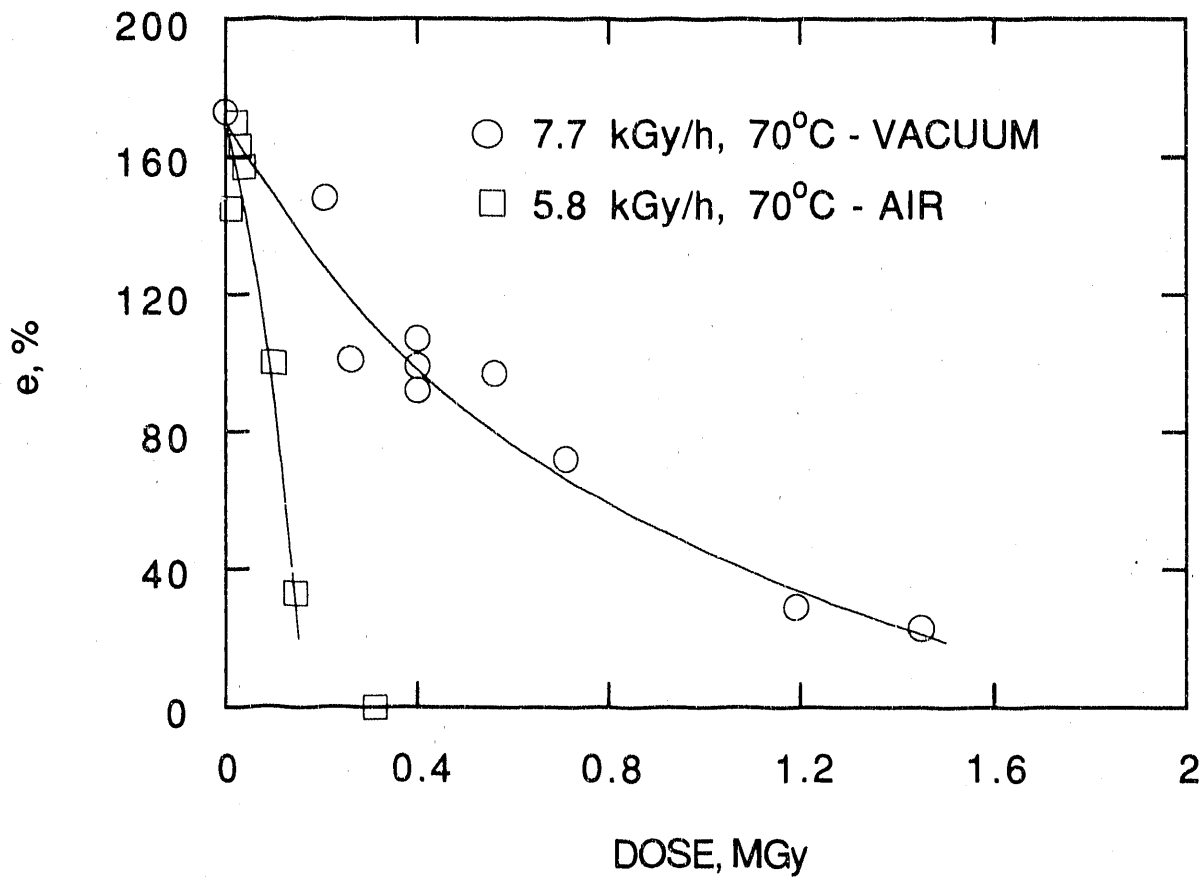

Fig. 12. Ultimate tensile elongation data for ETFE-A versus dose at 70°C plus 5.8 kGy/h in air (squares) and at 70°C plus 7.7 kGy/h in a vacuum environment (circles).

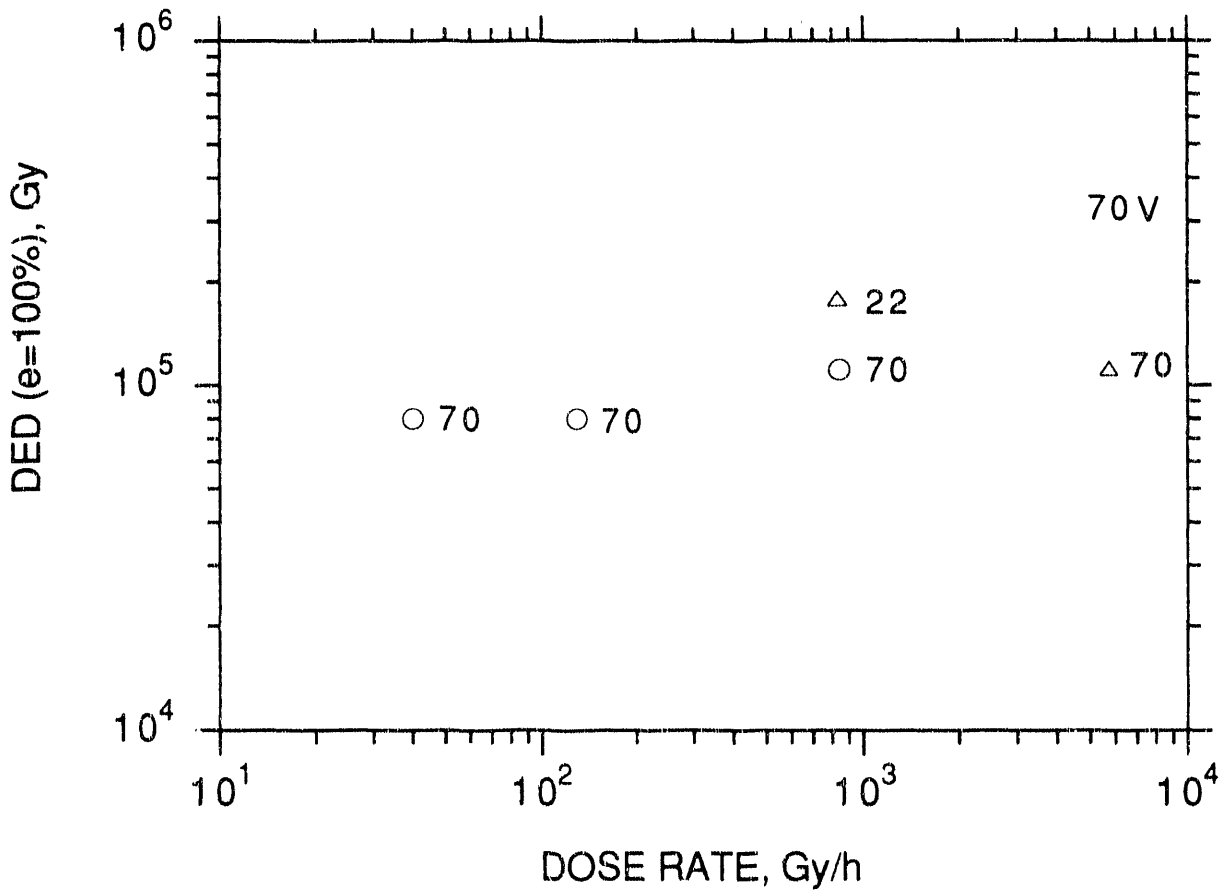

Fig. 13. Radiation dose required for the ultimate tensile elongation of ETFE-A to decrease to 100% absolute at various combinations of dose rate and temperature (the numbers by the data points give the temperature in °C). Aging conditions that likely result in homogeneously oxidized materials are plotted as circles; the data points plotted as triangles represent aging conditions where important diffusion-limited oxidation effects are suspected. The experiment conducted under vacuum conditions is plotted as a V.

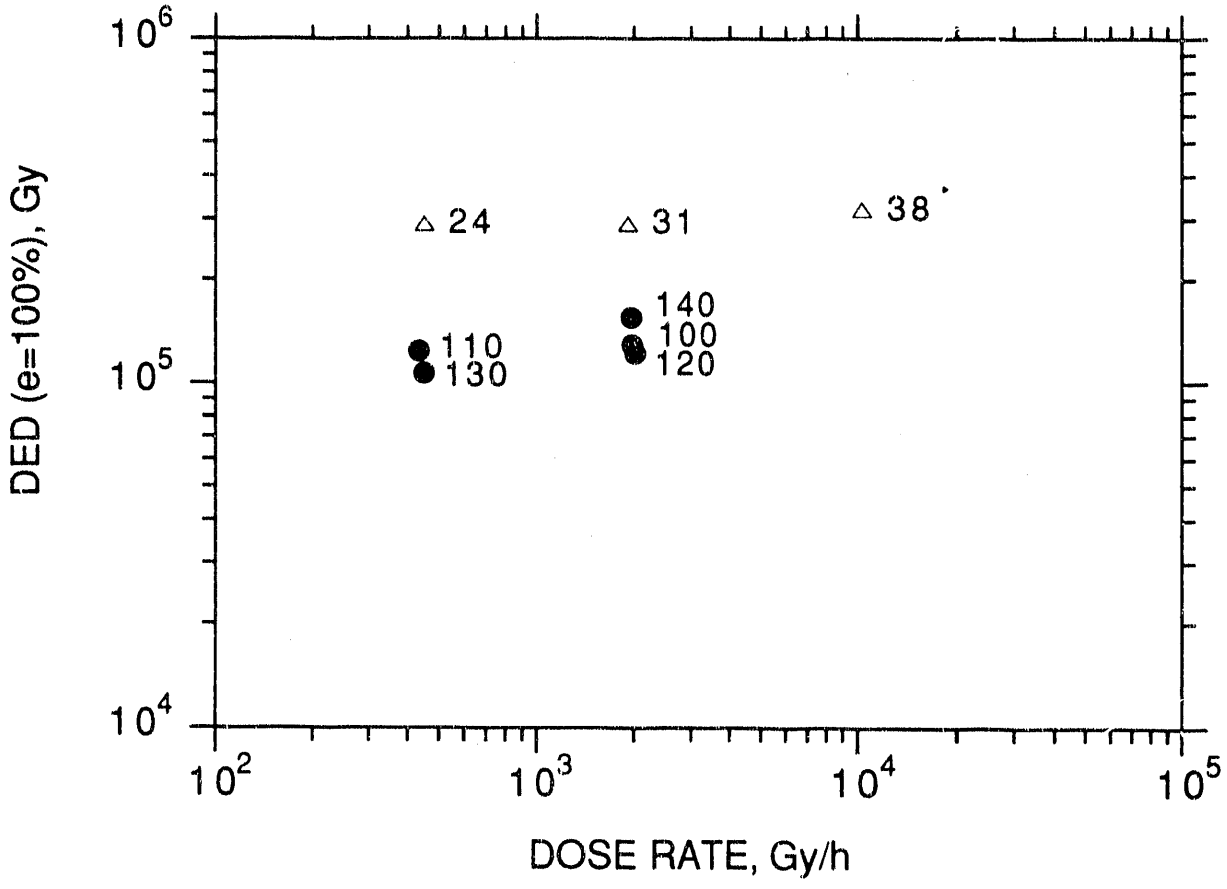

Fig. 14. Radiation dose required for the ultimate tensile elongation of ETFE-B to decrease to 100% absolute at various combinations of dose rate and temperature (the numbers by the data points give the temperature in °C). Aging conditions that likely result in homogeneously oxidized materials are plotted as filled circles; the data points plotted as triangles represent aging conditions where important diffusion-limited oxidation effects are suspected.

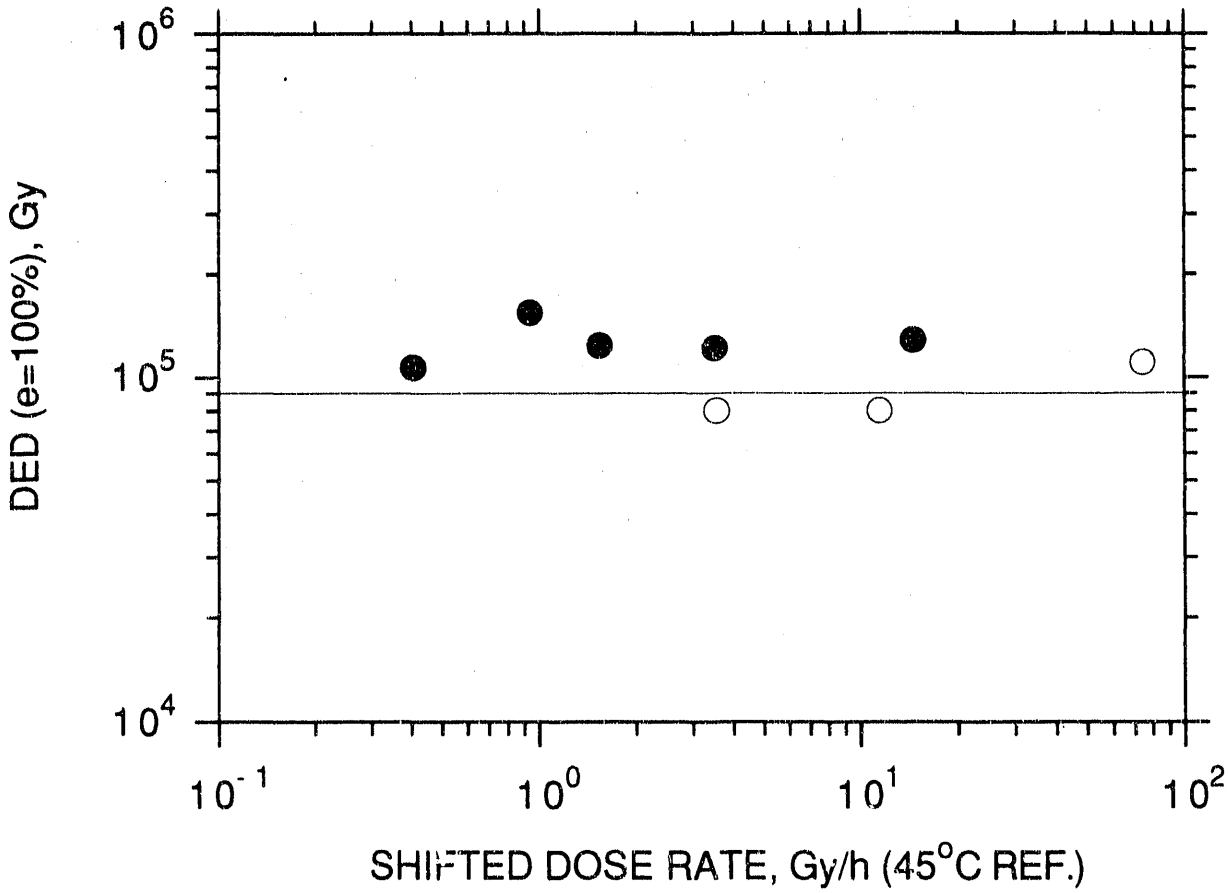

Fig. 15. Resulting ETFE predictions at 45°C after the data points corresponding to homogeneously oxidized materials in Figs. 13 (open circles) and 14 (closed circles) were shifted using the time-temperature-dose rate superposition methodology. An activation energy of 21 kcal/mole was assumed.

degradation begins for radiation-aged ETFE materials, the elongation tends to drop precipitously, as illustrated for the air-aged results in Fig. 12. More gradual drops in elongation are found for other materials; for instance, elongation versus dose curves for the two hypalon materials studied above tend to approximate the shapes observed for thermal-only exposures in Figs. 7 and 10. Thus, the 100% absolute elongation results for ETFE represent close to the end of useful lifetime, whereas significant additional life might exist for hypalon materials after reaching this criterion.

Silicone Insulation

The silicone insulation material was aged under combined radiation-thermal conditions ranging from approximately 25 to 5000 Gy/h at temperatures up to 130°C. Under each combined-environment condition, the ultimate tensile elongation data were obtained versus aging time and used to estimate the dose required for the elongation to decrease to various levels from its initial value (e_0) of 420%. Figure 16 gives data which represent the dose required for e/e_0 to reach 0.5 versus the dose rate and temperature conditions. Because of the relatively high oxygen permeation constants appropriate to silicone materials, [13] all of our experimental conditions are predicted to result in homogeneously oxidized samples. The general trend of the data indicates the presence of a chemical dose-rate effect, since raising the temperature or lowering the dose rate tends to increase the degradation rate per unit dose. It is apparent, however, that some of the results are unusual. For instance, the degradation rate of the tensile elongation is slightly faster at 42°C plus ~50 Gy/h then at 61°C plus ~50 Gy/h. This could be a real phenomenon, reflecting a diminished chemical degradation rate as the temperature is raised. On the other hand, it more likely reflects subtleties in the relationship between the conveniently chosen degradation parameter (elongation) and the underlying degradation chemistry. The expected trend (an increase in degradation rate as the temperature is increased) occurs at higher temperatures and completely dominates this small aberration. Even so, the presence of such aberrations coupled with the relatively small number of combined-environment experiments makes it difficult to accurately determine an activation energy using the procedure outlined in Fig. 5. However, as mentioned above in the discussion of the ETFE results, all previous empirically determined activation energies appropriate to time-temperature-dose rate superposition are equal to~ 21±4 kcal/mol. Since ~21 kcal/mol is also found [16] to be appropriate for the thermal activation energy of a nuclear power plant silicone insulation material, we will again choose an activation energy of 21 kcal/mol to shift the data of Fig. 16 to a reference temperature of 45°C. The results, plotted as the open circles in Fig. 17, are reasonably superposed. Also shown as the filled circles are shifted data at 100% absolute elongation. The enhanced scatter for this damage level appears to be random since there is no obvious trend with the combined-environment temperatures. For aging conditions of 0.1 Gy/h plus 45°C, these results imply that the elongation will drop to 100% absolute after ~50 years.

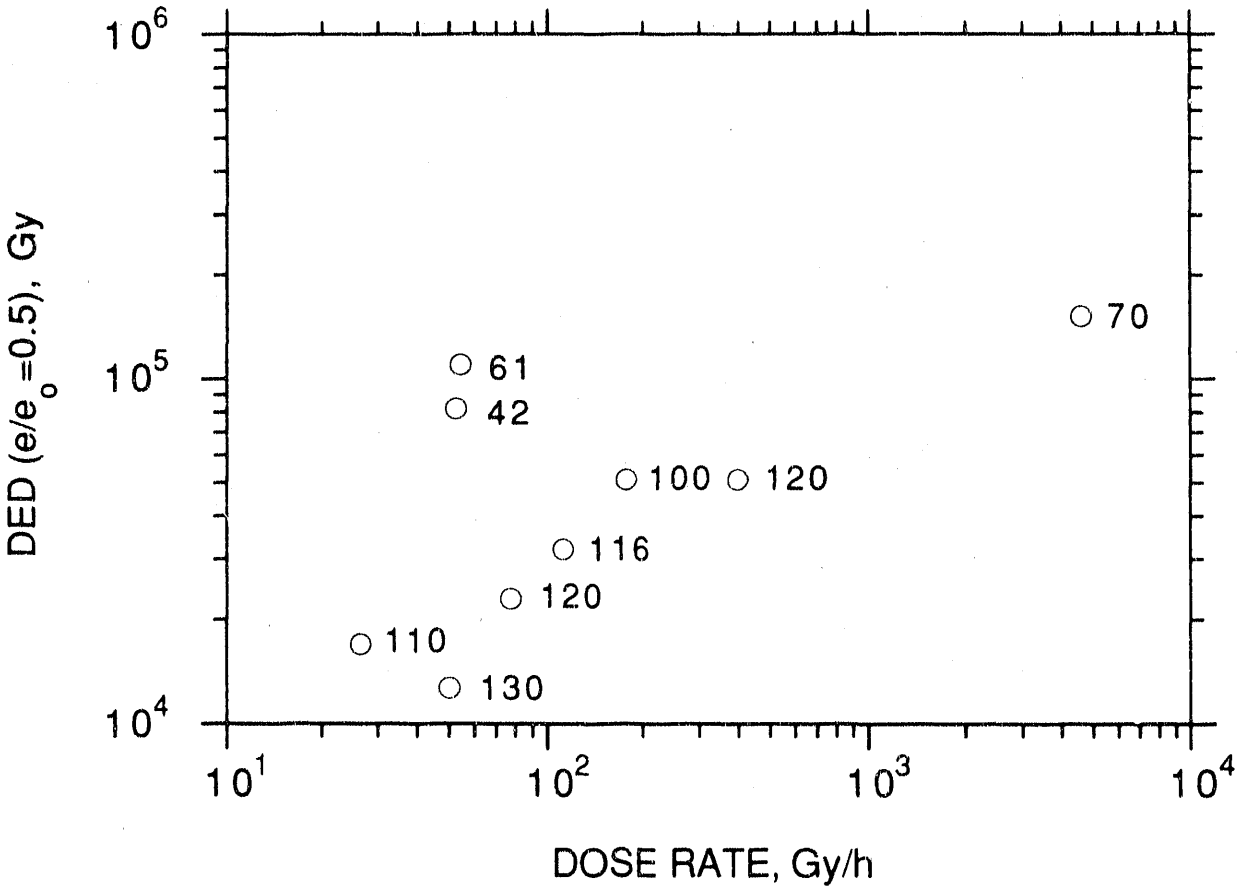

Fig. 16. Radiation dose required for the ultimate tensile elongation of the silicone rubber insulation material to decrease to 50% of its initial value at various combinations of dose rate and temperature (the numbers by the data points give the temperature in °C).

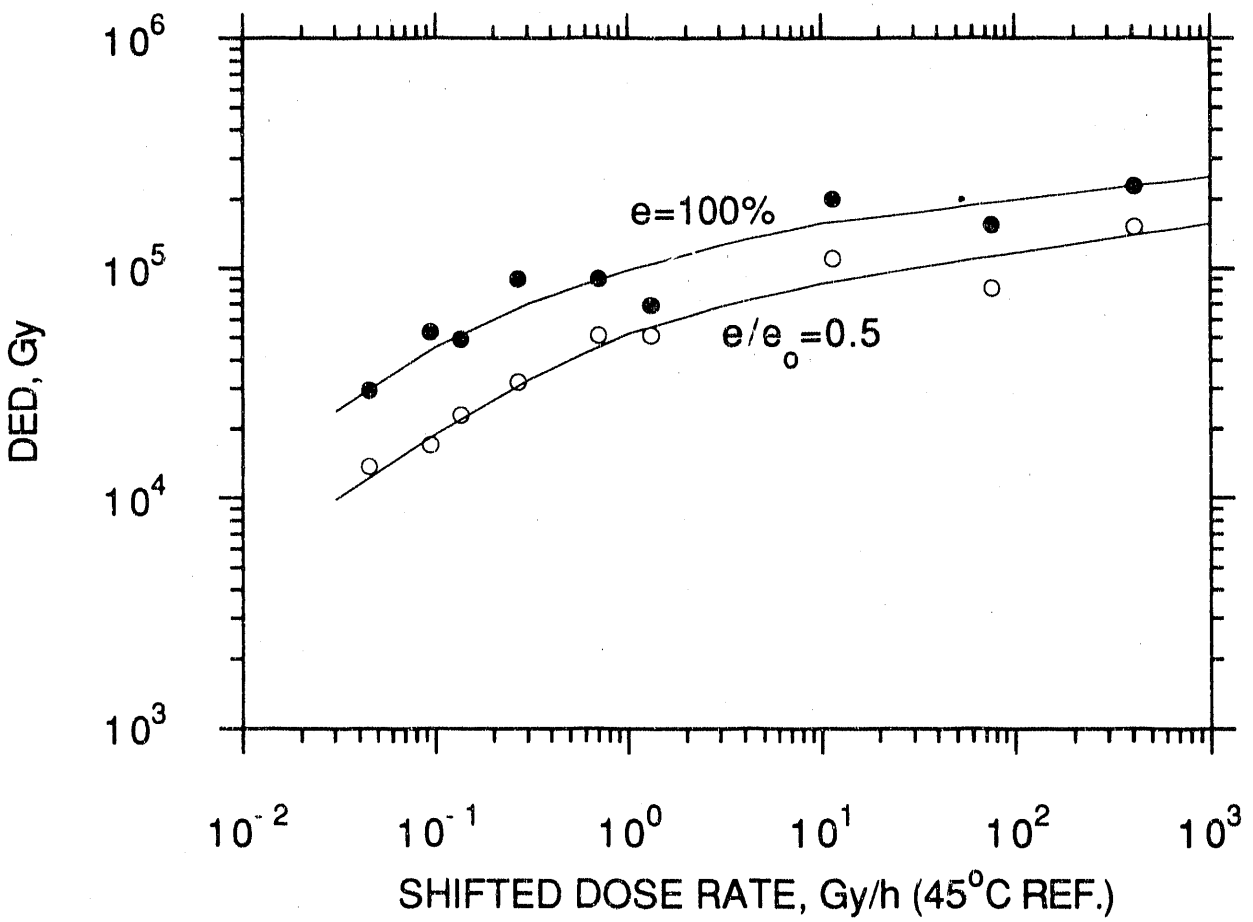

Fig. 17. Predictions, for the silicone rubber insulation material, of the dose required for the ultimate tensile elongation to drop to 50% of its initial value (open circles) and to 100% absolute (closed circles) versus dose rate at 45°C. The data points of Fig. 16 and similar results at 100% absolute elongation were time-temperature-dose rate shifted according to the methodology assuming a 21 kcal/mol activation energy.

COMPARISON OF MODEL PREDICTIONS WITH LONG-TERM DATA

In this report and the previous document, [3] we have used the ideas underlying the time-temperature-dose rate superposition approach to generate predicted degradation results down to very low dose rates for a number of important nuclear power plant cable jacketing and insulation materials. Once the aging environment appropriate to a material is specified, the results from the modelling allow us to predict its long-term degradation. The only reliable means of confirming the model predictions is direct comparison with samples which have been aged at low dose rates for long periods of time, preferably in a nuclear power plant environment. This approach was tested in the previous report for the PVC and low density polyethylene materials, where the degradation found for samples exposed at the Savannah River reactor to 12 years of 0.2 Gy/h plus 43°C was shown to be in excellent agreement with model predictions from the time-temperature-dose rate superposition method.

Ideally, comparisons of model predictions with cable materials which have been aged for extended time periods in real nuclear environments should involve the identical commercial formulation. This is usually impossible since the unaged materials needed for the required combined-environment, accelerated exposures are normally unavailable when decades-old, ambiently aged materials are recovered from a plant. In some fortunate cases, identical materials kept in a benign environment (e.g., on a roll in storage or at ambient temperature with no electrical loading) are available; these can be approximated as "unaged" material and used in the accelerated simulations. This approach was applied to the PVC and low density polyethylene materials from Savannah River. In the absence of sufficient quantities of the identical, unaged material, it may still be possible to make comparisons based on the generic class of materials. In other words, if modelling predictions on a large number of generic materials were available and these predictions were in reasonable accord, one could test the range of predictions against an ambiently aged material of the same generic type. Consistency with the range of predictions would give enhanced confidence both in the modelling and in the generic application of the predictions. For these reasons, it would be desirable (1) to generate modelling results on numerous commercial formulations for each important generic group of materials and (2) to obtain as many long-term, ambiently aged results as possible. In this section, we apply these ideas by showing that, within generic classes of materials examined to date, there is a reasonable consistency between our limited modelling results and some limited, long-term aging results.

Hanford Hypalon Material

Some years ago, we were able to obtain two samples of a hypalon insulation material which had been aged for more than 14 years in the Hanford N-Reactor, starting in early 1964. A 20-foot cable sample came from the top of the reactor (+40 foot elevation) and a 16-inch cable

sample came from under the reactor. Based on actual monitoring of the two locations, [17] it was estimated that during the ~7.5 years of integrated reactor operation, the environments averaged 0.021 Gy/h (primarily gamma) at 48°C and 1.1 Gy/h (primarily neutron) at 33°C, respectively. Since the dose rates were 25 to 50 times lower and the temperatures were close to ambient during the ~7 years of reactor shutdown, degradation during these periods is assumed to be minimal. We also obtained a small section of identically manufactured, unused cable which had been stored at room temperature for the 14 year period. Based on our thermal aging studies of the two hypalon materials (Figs. 7 and 10) in the present paper and the earlier hypalon material [2,3], we conclude that these storage conditions would cause no measurable changes in mechanical properties for this material. We therefore consider this piece of cable to represent essentially new material and hence use its properties as a benchmark for determining the changes which have occurred for the two sections of cable aged for 7.5 years under reactor conditions. For the new material, the ultimate tensile elongation (e) of the hypalon insulation was found to equal 450% ± 20%. Values of e for the insulations aged on top of and under the reactor were 395% ± 30% and 445% ± 20%, respectively, indicating that only minor mechanical deterioration had occurred under the reactor environments estimated above.

To assess how well modelling predictions for the three hypalon materials studied to date agree with the 7.5 year data for the Hanford material, we use the modelling results to generate predicted elongation versus time curves for the three modelled materials under the two aging conditions appropriate to the Hanford materials. The resulting plots, corresponding to environments of 0.021 Gy/h plus 48°C and 1.1 Gy/h plus 33°C are shown in Figs. 18 and 19, respectively. Although the rates of degradation for the three hypalon materials vary somewhat, the shapes of the curves are quite similar. Given that the three hypalons were formulated for very different purposes (an outside jacket, an internal thin jacket and an insulation), these results offer preliminary evidence that most other commercial hypalon materials might be expected to have similar magnitudes and shapes for their degradation behaviors. As more hypalons are investigated in the future, more confidence in such generic conclusions will be possible. In addition, the more generic information which exists on a particular material, the easier it will be to confirm that a new material is "generically consistent", since confirmation should be possible with a minor number of well-chosen accelerated degradation conditions.

The actual results for the Hanford hypalon materials can now be compared to the modelling predictions for the three hypalon materials; these are plotted as the crosses at 7.5 years on Figs. 18 and 19. It is clear that the results for the plant-aged materials from Hanford are consistent, within the experimental uncertainties, with the range of results predicted from the modelling. Considering the observation that the Hanford material was installed in the early 1960's and therefore represents an early commercial formulation, the consistency of the results for the various hypalon materials and the resultant lifetime

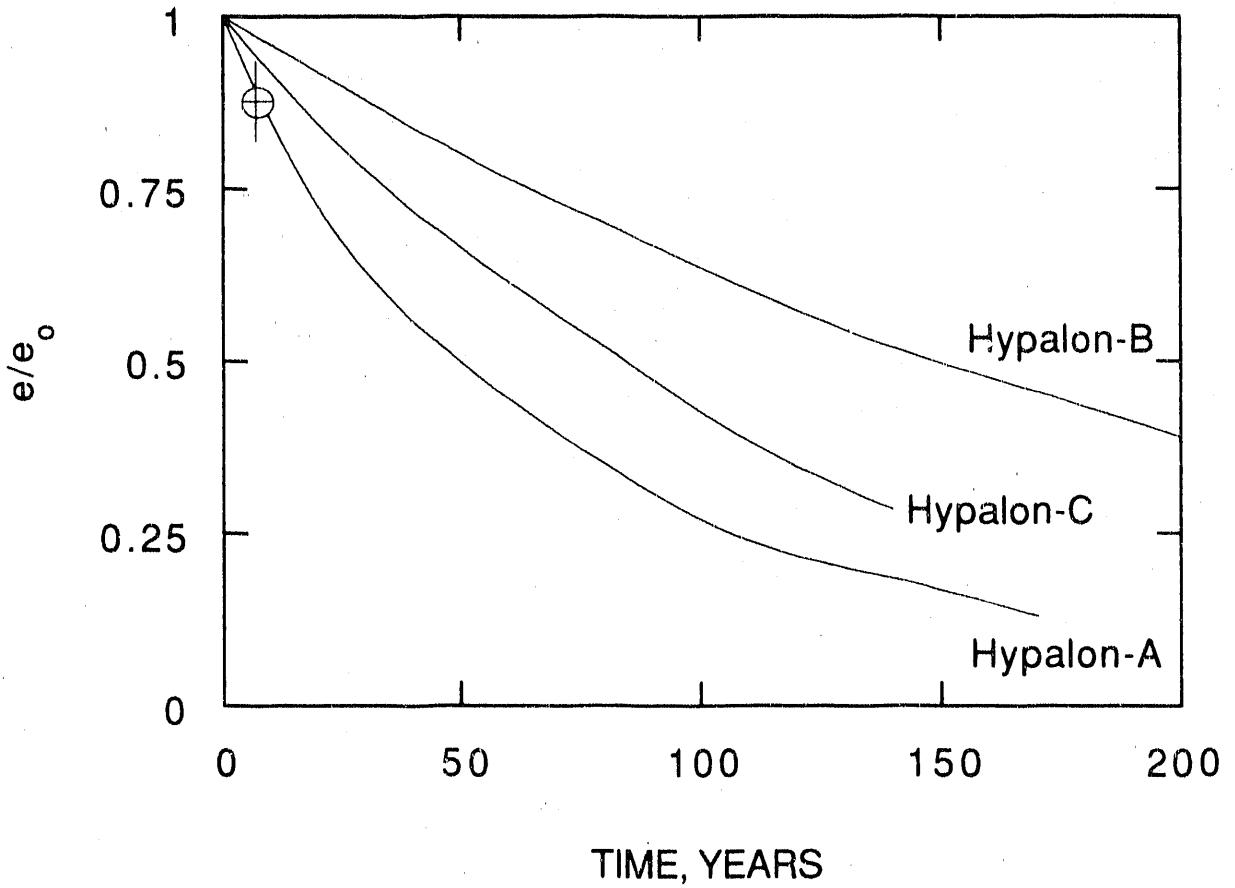

Fig. 18. Predictions at 0.02 Gy/h plus 48°C for the three hypalon materials studied in this and the previous report. [3] The predictions are derived from the time-temperature-dose rate superposed results for the three materials. The point plotted at 7.5 years represents data measured on another commercial hypalon material which had experienced 7.5 years of aging under estimated aging conditions of 0.02 Gy/h plus 48°C.

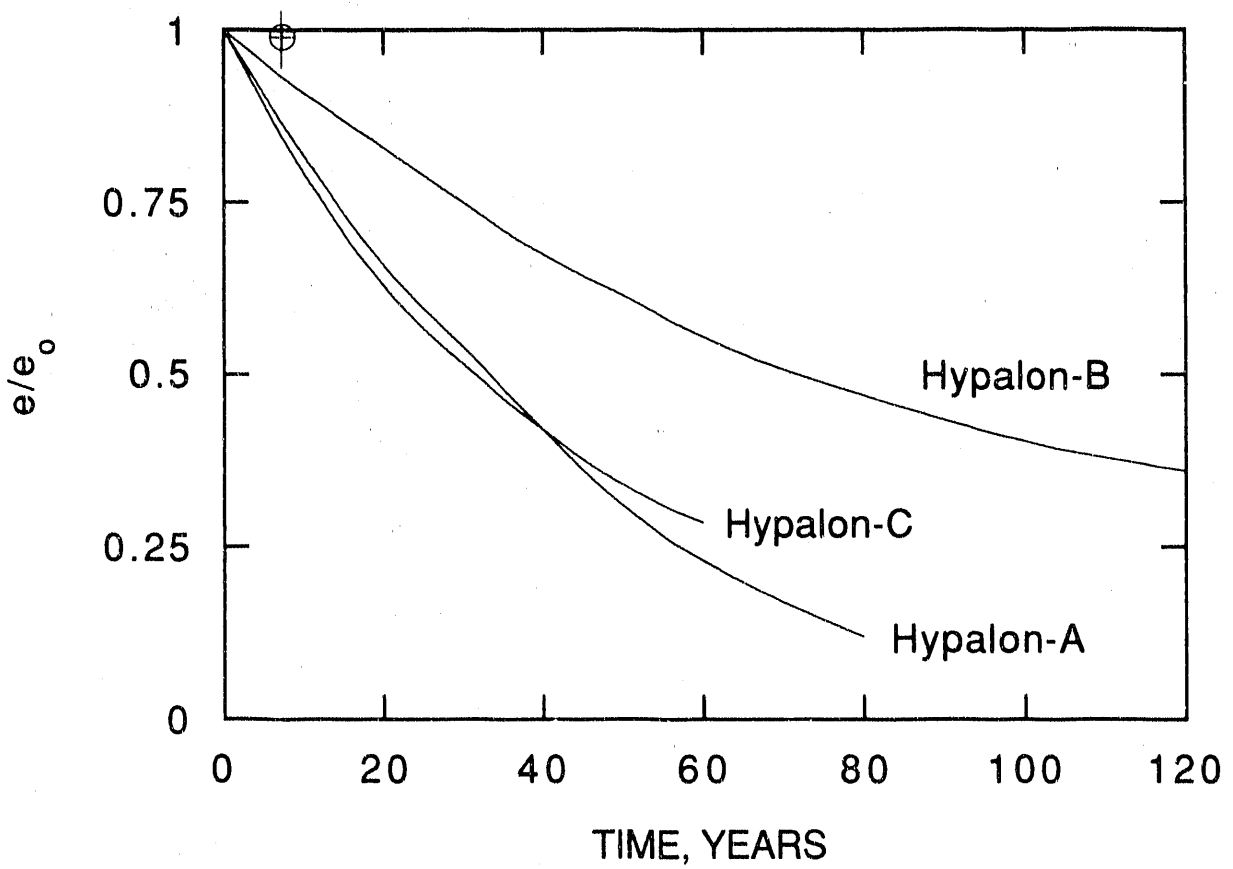

Fig. 19. Predictions at 1.1 Gy/h plus 33°C for the three hypalon materials studied in this and the previous report. [3] The predictions are derived from the time-temperature-dose rate superposed results for the three materials. The point plotted at 7.5 years represents data measured on another commercial hypalon material which had experienced 7.5 years of aging under estimated aging conditions of 1.1 Gy/h plus 33°C.

implications are rather encouraging. For instance, Fig. 19 implies that most hypalon materials should remain flexible after 60 years in a rather severe radiation environment.

Siemens Studies [18]

Recently, Rost and co-workers [18] reported on a continuing study which is investigating the radiation resistance in a gamma source and in a PWR containment of a number of cable jacketing and insulation materials under dose rate conditions ranging from highly accelerated (~10^4 Gy/h) to extremely low (<1 Gy/h). Their long-term studies, which have now been running for 9 years, include results for a number of materials which are similar to the materials modelled in our accelerated experiments. The purpose of this section is to show that within generic groups of materials, the results from their long term exposures are consistent with the curves predicted from our modelling.

In their studies, Rost and coworkers [18] monitored the ultimate tensile elongation versus dose and dose rate for a number of materials, including a plasticized PVC, three ETFE's, three silicone rubbers (SiR) and a crosslinked polyethylene (XPE). Their recent report summarizes the dose required for the ultimate tensile elongation to decrease to 50% of its initial value; these results are summarized in Table 2. Except for the experiments conducted in the PWR (estimated temperature of 50°C), all of the other experiments were carried out at ambient temperature, which we will assume averages 22°C. Dose-rate effects are evident for every generic material in the Table. Based on our extensive studies of diffusion-limited oxidation, [5-11] we feel it is likely that diffusion-limited artifacts are present for their PVC and ETFE materials at the two highest dose rates (10^4 Gy/h and 450 Gy/h) and for their XPE material at the highest dose rate (10^4 Gy/h). Diffusion effects may also be present for some of the other "short-term" conditions as noted by us in the Table. Although we are interested in the remaining data in the Table (e.g., the data likely taken on homogeneously oxidized samples), our main interest is in comparing the long-term PWR data taken at 50°C and 0.7 Gy/h with our time-temperature-dose rate extrapolated predictions at this condition. The PVC, ETFE, silicone rubber and crosslinked polyethylene materials studied by Rost and co-workers [18] come from different manufacturers compared to the materials used to generate our low-dose-rate predictions, and therefore represent formulations which differ in unknown ways. Even so, one might hope for and perhaps anticipate reasonably similar degradation behaviors for different commercial formulations of each generic material.

We first compare the long term data of Rost on PVC with our time-temperature-dose rate superposition predictions for a similar material. We found that an activation energy of 23 kcal/mol led to excellent superposition of combined-environment PVC data analyzed using the procedures outlined in Fig. 5 and that the resulting dose-rate curves could be quantitatively modelled from a chemical kinetic treatment [3,5]. The earlier analyses derived dose-rate predictions at 43°C for

TABLE 2

Summary of Siemen's Results [18]

Material	Dose to $e/e_o = 0.5$ in Gy at				
	10^4 Gy/h R.T. γ	400-500 Gy/h 22°C[a] γ	40-50 Gy/h 22°C[a] γ	1.3-0.5 Gy/h 22°C[a] γ	0.7 Gy/h 50°C PWR
SiR I	6×10^5 [c]	1.7×10^5	1.7×10^5	5×10^4	4×10^4
SiR II	5.5×10^5 [c]	1.6×10^5	1.8×10^5	5×10^4	4×10^4
SiR III		1.6×10^5	1.6×10^5	(8×10^4)[a] $e/e_o = 0.65$ after 5.4×10^4	4.5×10^4
PVC	$>2\times10^6$ [b]	3×10^5 [b]	2×10^5	5×10^4	3×10^4
ETFE I	4×10^5 [b]	1.5×10^5 [b]	1.5×10^5 [c]	$e/e_o = 0.9$ after 5.4×10^4	4.5×10^4
ETFE II		1.7×10^5 [b]	1.7×10^5 [c]	$e/e_o = 0.9$ after 5.4×10^4	$e/e_o = 0.8$ after 4.2×10^4
ETFE III		1.5×10^5 [b]	1.5×10^5 [c]	no decrease after 5.4×10^4	no decrease after 4.2×10^4
XPE	2×10^6 [b]	6×10^5 [c]	6×10^5	no decrease after 5.4×10^4	no decrease after 4.2×10^4

[a] assumed for our analyses
[b] diffusion-limited oxidation effects likely (our assumption)
[c] diffusion-limited oxidation effects possible (our assumption)

e/e_o = 0.8, 0.6 and 0.4. Since we are now interested in comparisons with Rost's long-term data for a 50% drop in elongation at 50°C plus 0.7 Gy/h, our combined-environment PVC data have been reanalyzed at e/e_o = 0.5 and shifted to 50°C using the 23 kcal/mol activation energy. The shifted results are plotted as circles in Fig. 20; the curve through the data represents the theoretical fit at 50°C, derived from the underlying kinetics. [5] The long-term PVC results of Rost and co-workers from Table 2 can now be compared with our predictions. The ~5 year PWR result at 50°C is plotted directly on Fig. 20 as the square at 0.7 Gy/h; it is clearly in excellent agreement with the model predictions. Rost's room temperature data points at 0.9 Gy/h and 45 Gy/h can be shifted to 50°C (e.g., to the right) using the 23 kcal/mol activation energy; the results are given by the two right-hand squares shown in the figure. Even though two different PVC formulations are involved in the comparisons, both the shape and the positioning of the dose-rate effects are similar. This instills further confidence in the time-temperature-dose rate superposition approach and offers some early evidence of generic behavior for PVC materials.

In Fig. 17 we derived the 45°C time-temperature-dose rate superposed curve for our silicone insulation material at e/e_o = 0.5 assuming a 21 kcal/mole activation energy. To compare these predictions with the Siemen's silicone data, we shift our results to a 50°C reference temperature, yielding the curve shown in Fig. 21. The Siemen's data for three silicone rubber materials are plotted on the same figure, with their long-term 50°C points plotted directly at 0.7 Gy/h and their room temperature data plotted after shifting to 50°C using the same 21 kcal/mol activation energy. Excellent consistency exists between the model predictions and the long-term data. Again, both the modelling and the long-term results reach similar conclusions concerning the increase in degradation rates at nuclear power plant aging conditions compared to typical accelerated aging exposure conditions. The generic similarities of the three Siemens materials and the correspondence between the dose-rate results for these materials and the modelling predictions for our silicone offer some evidence for the reasonableness of our 21 kcal/mole activation energy assumption.

Earlier we had concluded that, when homogeneously oxidized, our two ETFE materials showed little evidence of dose-rate or temperature effects and that low-dose-rate exposures would result in significant degradation after ~$9\pm3\times10^4$ Gy total dose. For the three Siemen's ETFE materials (see Table 2), the higher-dose-rate gamma exposures at ~22°C imply that e/e_o reaches 0.5 after 4×10^5 Gy at 10^4 Gy/h (diffusion anomalies assured) and after ~1.6×10^5 Gy at both 450 Gy/h (diffusion likely) and 45 Gy/h (diffusion possible). Under the low-dose-rate, long-term exposures, two of the three materials have not reached this level of damage after greater than ~5×10^4 Gy (9 years) at both the 22°C and 50°C exposure temperatures. The third ETFE material may have just reached this damage level after ~4.5×10^4 Gy at 50°C, but has not at 22°C. Under the homogeneous oxidation conditions expected at low dose rates, all three materials should reach e/e_o = 0.5 at doses less than the ~1.6×10^5 Gy found at 45 and 450 Gy/h. Thus the dose to significant

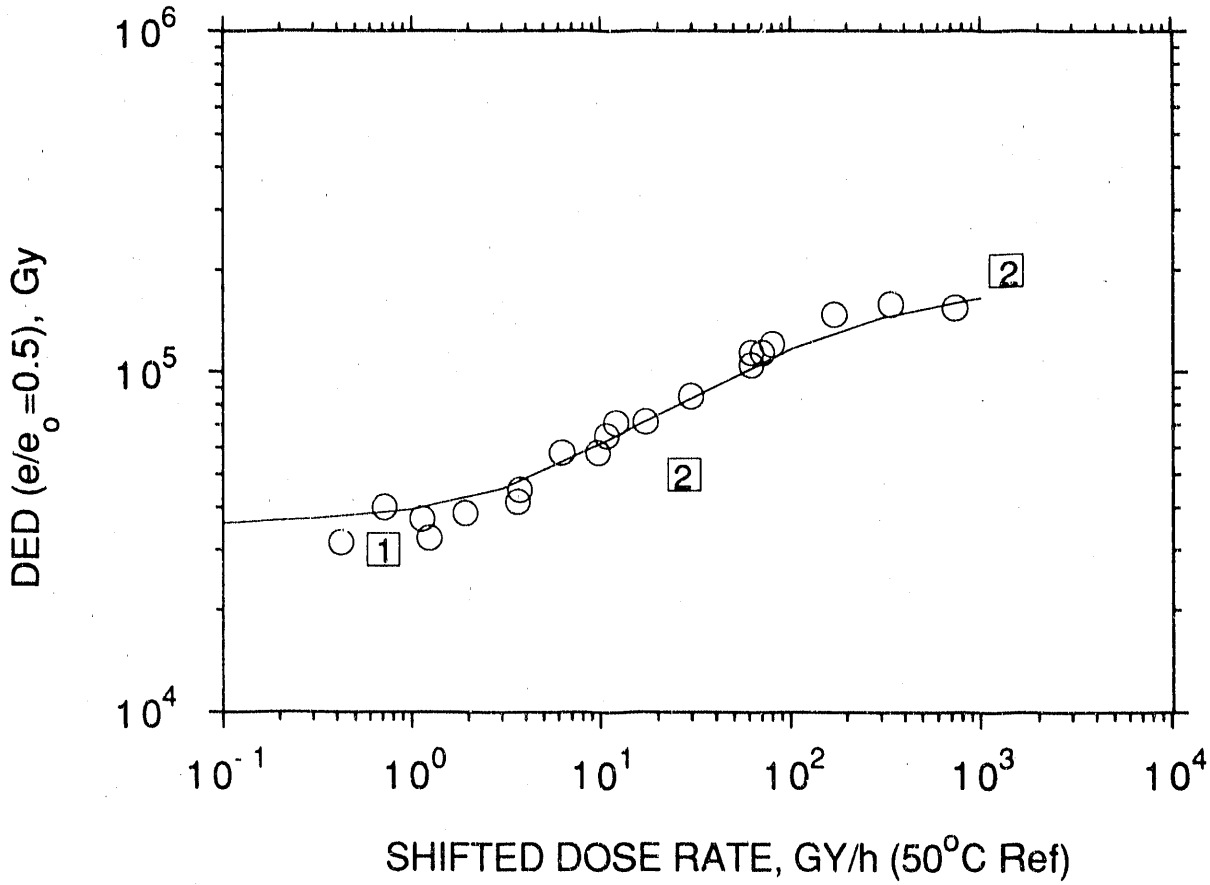

Fig. 20. The circles give PVC results (for a 50% drop in ultimate tensile elongation) which have been time-temperature-dose rate superposed at a 50°C reference temperature using a 23 kcal/mol activation energy. The S-shaped curve drawn through these data comes from the theoretical kinetic modelling of the chemical mechanism responsible for the dose-rate effect in this material. [3,5] For comparison, a long-term result [18] for a second (different) PVC material which had been aged in a nuclear reactor environment at 50°C and 0.8 Gy/h is plotted as the square labelled with a 1. In addition, long to intermediate term gamma results for the second PVC material (see Table 2) are plotted as squares (labelled 2) after time-temperature-dose rate shifting of these results from ambient temperature (assumed to be 22°C) to the 50°C reference temperature.

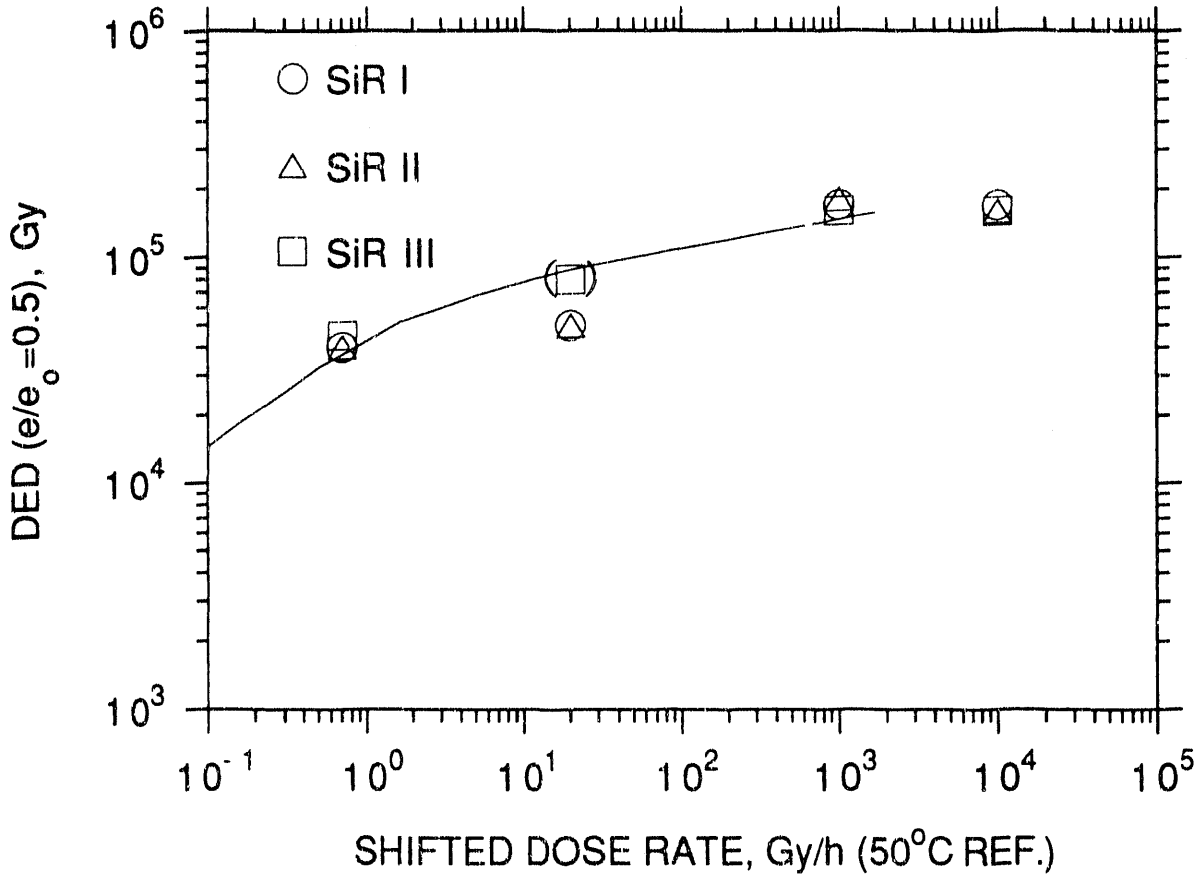

Fig. 21. Solid curve gives predicted modelling results at $e/e_o = 0.5$ for silicone rubber material at 50°C. The three data points plotted at 0.8 Gy/h represent long-term nuclear power plant aging results at 0.8 Gy/h plus 50°C for three different commercial silicone rubber insulation materials studied by Siemens. [18] The long to intermediate term gamma results from Siemens (Table 2) are also plotted after time-temperature-dose rate shifting of these results from ambient temperature (assumed to be 22°C) to the 50°C reference temperature.

damage at low dose rates should be between 5 and 16×10^4 Gy for the ETFE materials studied by Siemens. This is in reasonable accord with our predicted result of $9 \pm 3 \times 10^4$ Gy. This conclusion, which hints at generic similarities among ETFE materials, is again not surprising, given the lack of significant additives used in various commercial ETFE formulations.

In our previous report, we analyzed some limited combined-environment data for a chemically crosslinked polyethylene material; the lack of dose-rate and temperature effects, when analyzed using the time-temperature-dose rate superposition approach, led us to the prediction that dose-rate effects should be unimportant at least down to ~10 Gy/h. After eliminating the high dose-rate experiment which we estimate was likely influenced by diffusion effects, we conclude that the crosslinked polyethylene data of Rost, et. al. [18] show no evidence of a dose-rate effect down to 0.7 Gy/h. This preliminary comparison (no degradation has occurred for the long-term data out to 9 years) again hints at an apparent consistency between the modelling and long-term data.

CONCLUSIONS AND APPLICATION OF APPROACH TO SAFETY-CABLE LIFE PREDICTIONS

In this report and the previous report, [3] we have shown that important dose-rate effects (both physical and chemical) exist for many polymeric materials. These effects make it very complicated to predict material lifetimes from high-dose-rate accelerated simulations. It appears, however, that our proposed time-temperature-dose rate superposition approach for analyzing combined-environment aging results now offers a useful method for predicting lifetimes of polymeric materials exposed to long-term, low-level radiation environments. In addition, results from modelling and long-term power plant exposures on different formulations of a number of generic types of materials offer preliminary evidence that reasonably similar degradation rates and time dependencies might occur for many generic materials. If such generic behaviors can be more extensively documented, it should help establish those materials expected to be little affected by long-term aging in nuclear plants.

Although most of our time-temperature-dose rate superposition analyses have concentrated on making predictions versus dose rate at one isothermal temperature (usually near 45°C), the modelling allows the results to be easily transformed to other temperatures of interest. In order to use the modelling for quick assessments of expected material behavior versus various aging conditions, it is particularly useful to plot the time required for the elongation to drop to a specified value (e.g., the time to equivalent damage or TED) versus dose rate and temperature. For example, Fig. 22 plots the time required for the elongation of the hypalon-B insulation material to drop to 100% absolute versus dose rate at four temperatures in the range of possible interest to nuclear power plant aging environments. The plots are appropriate to homogeneously oxidized material and therefore are not extended to high dose rates where diffusion-limited oxidation effects would be likely.

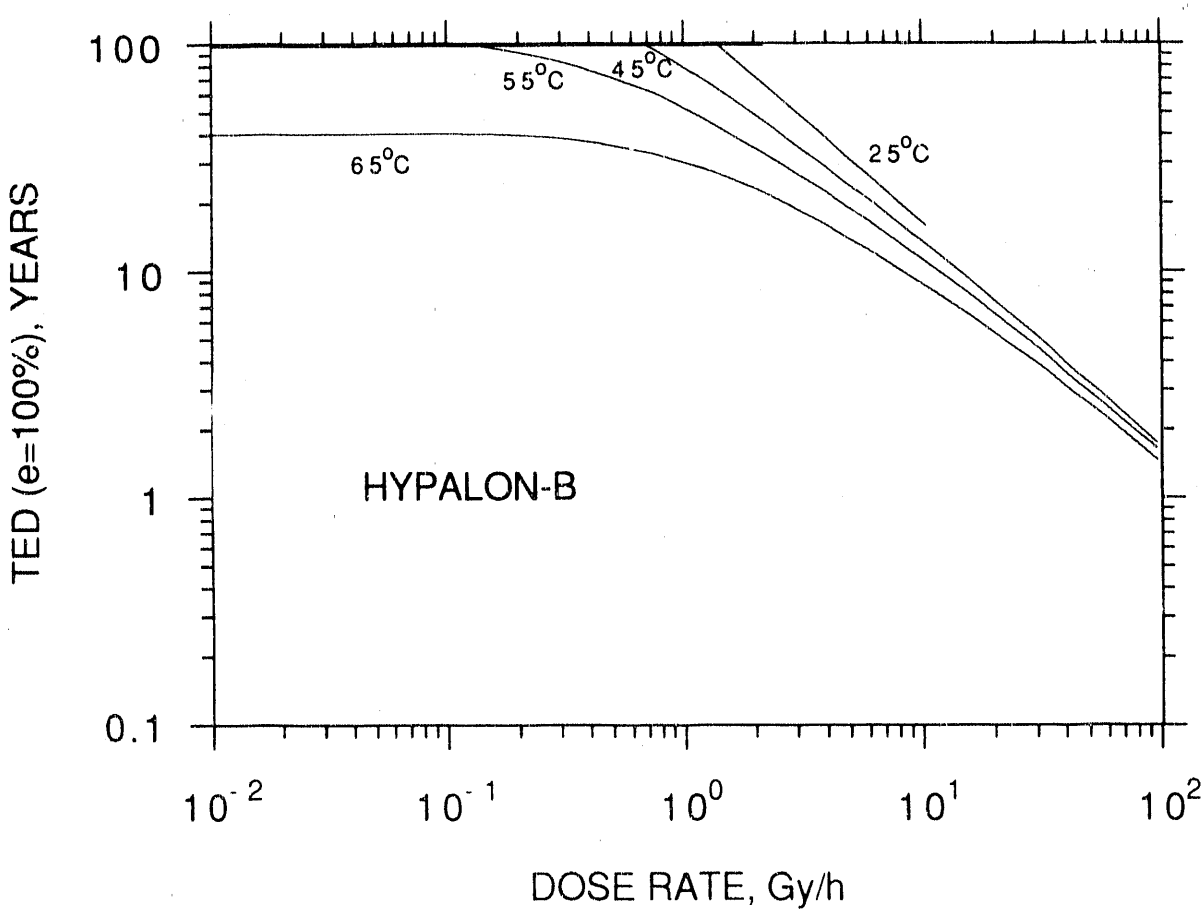

Fig. 22 Predictions for the hypalon-B commercial material (see Table 1) versus dose rate and temperature based on superposed model results. The time to equivalent damage (TED) refers to the predicted time required for the elongation to decrease to 100% absolute.

Although the 100% absolute elongation criterion used for this figure is an arbitrary choice, it represents a condition where the cable should still have sufficient flexibility to withstand the mechanical abuses associated with normal operation and maintenance. Thus the predictions shown in Fig. 22 can be considered conservative lifetime estimates. When the curves level out (slope of 0) at low dose rates (e.g., the 65°C curve), this reflects the transition to thermal-only domination of the degradation. When dose-rate effects are absent, the other limiting slope of -1 will occur. If a nuclear power plant contained this material and its worst estimated environment was 42°C and 1 Gy/h (100 rad/h), Fig. 22 would predict a "lifetime" greater than 80 years.

Figures 23-29 show similar plots at the 100% absolute elongation "lifetime" criterion for other materials modelled in this and in our previous reports. [3,5] These plots may be useful for estimating approximate lifetimes of the various materials and for making preliminary generic estimates on materials for which modelling results are not yet available. The shape of the various plots and their temperature dependencies reflect the importance and type of the underlying dose-rate effects. No explicit temperature dependence is shown for the ETFE results plotted in Fig. 26. In an earlier section of this paper, we tentatively concluded that dose-rate and temperature effects (at the low to moderate temperatures characteristic of nuclear power plant aging conditions) are minimal for homogeneously oxidized ETFE materials and that 90±30 kGy of radiation would be required for substantial degradation. This results in the two temperature-independent "bounding" lines having a slope of -1 (no dose-rate effects).

Although all the materials of Figs. 22-29 are compared at the same elongation level (100% absolute), the useful life beyond this point will depend strongly on the material. For instance, after this elongation is passed, the subsequent dropoff is relatively gentle for hypalon materials and quite abrupt for ETFE materials.

If the most severe aging environments in a typical nuclear power plant were determined to be ~45°C plus 0.1 Gy/h, the results from Figs. 22-29 indicate that, with the exception of the low density polyethylene and the neoprene, most materials should retain sufficient mechanical flexibility for 60 year exposures. It would of course be useful to have more modelling and long-term exposure results for additional commercial formulations of each generic material. This would be especially useful for the potentially suspect neoprene and low density polyethylene materials, since only one commercial formulation of each has been studied.

At this point, it is interesting to summarize some of our conclusions in Table 3, highlighting the magnitude of dose-rate effects which can result from a combination of physical and chemical effects. For each material studied, we list the approximate dose required to reach 100% absolute elongation under the following three experimental conditions:

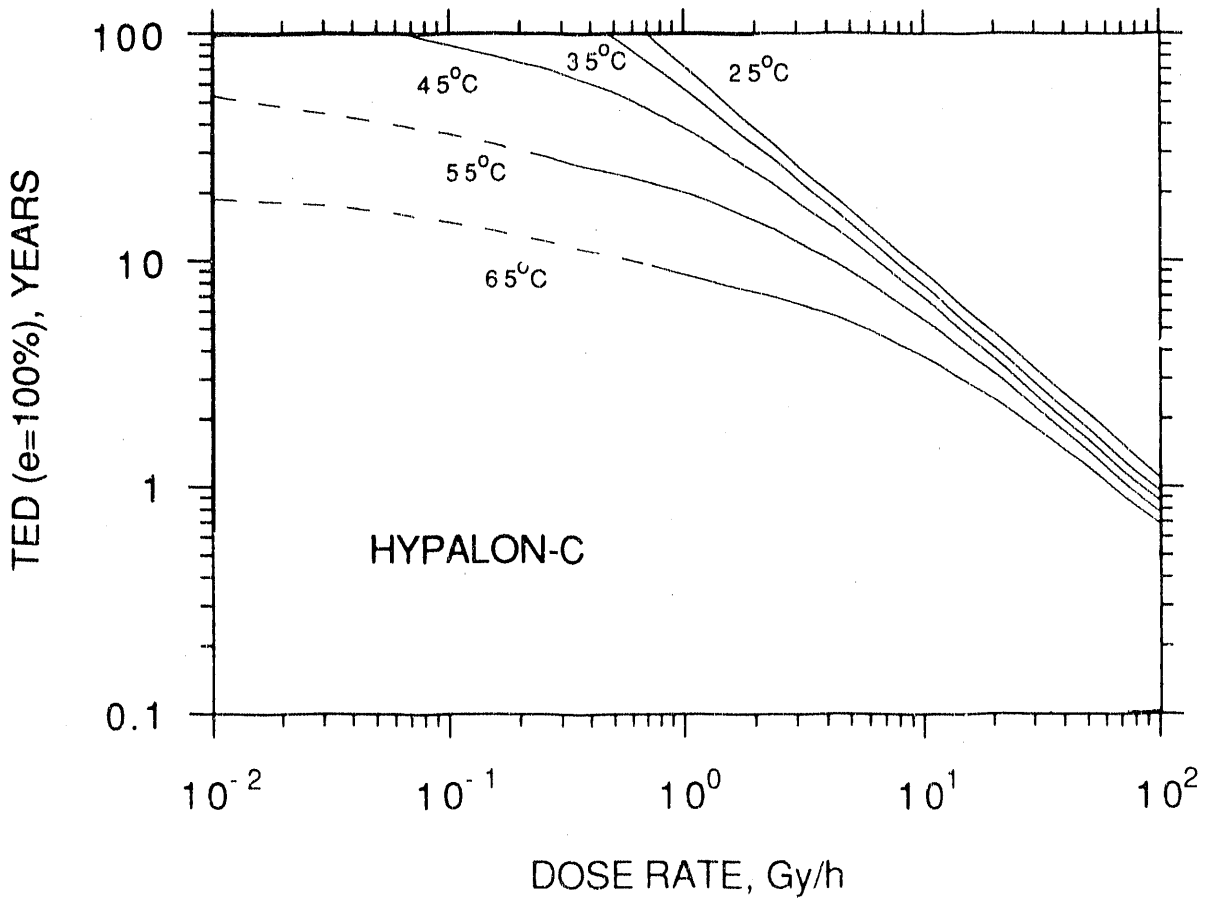

Fig. 23. Predictions for the hypalon-C commercial material (see Table 1) versus dose rate and temperature based on superposed model results. The time to equivalent damage (TED) refers to the predicted time required for the elongation to decrease to 100% absolute.

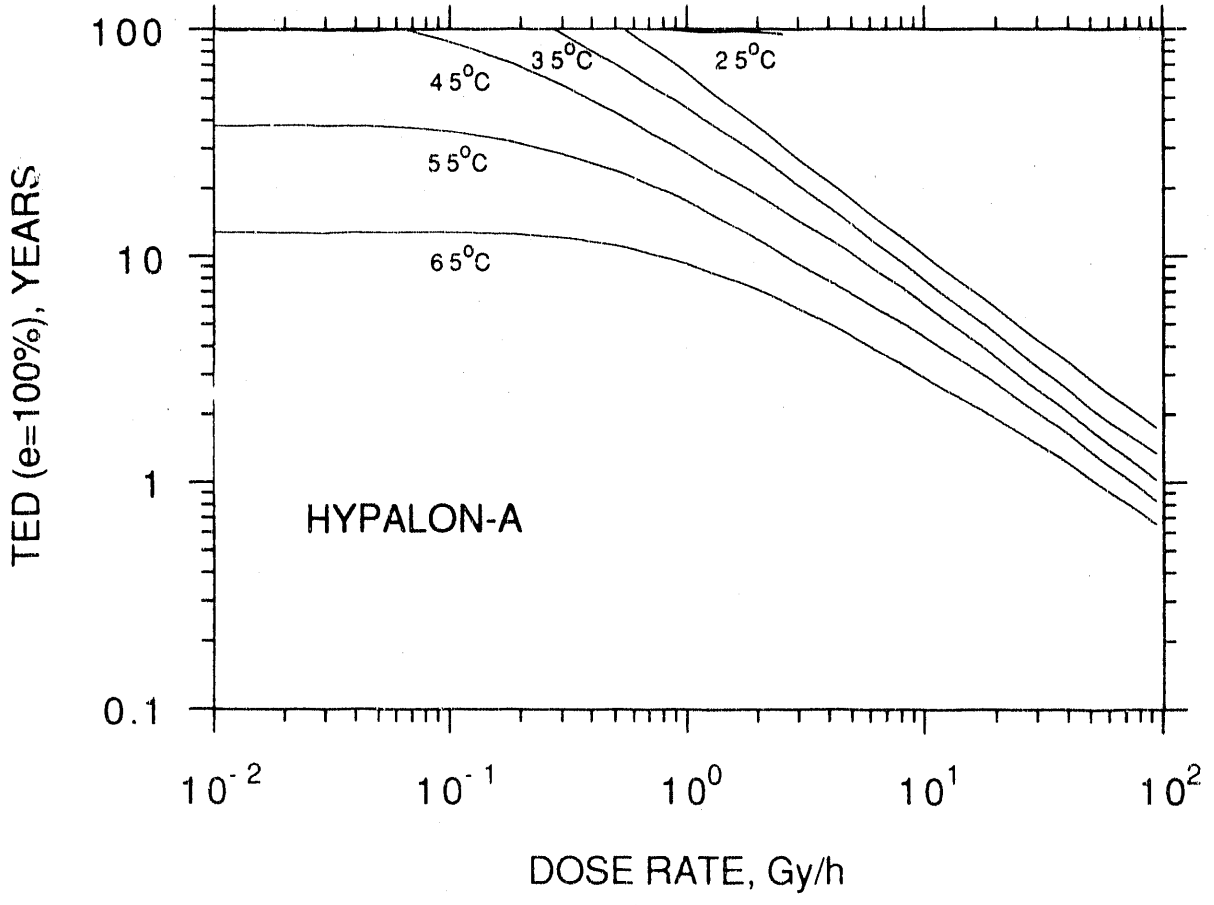

Fig. 24. Predictions for the hypalon-A commercial material (see Table 1) versus dose rate and temperature based on superposed model results. The time to equivalent damage (TED) refers to the predicted time required for the elongation to decrease to 100% absolute.

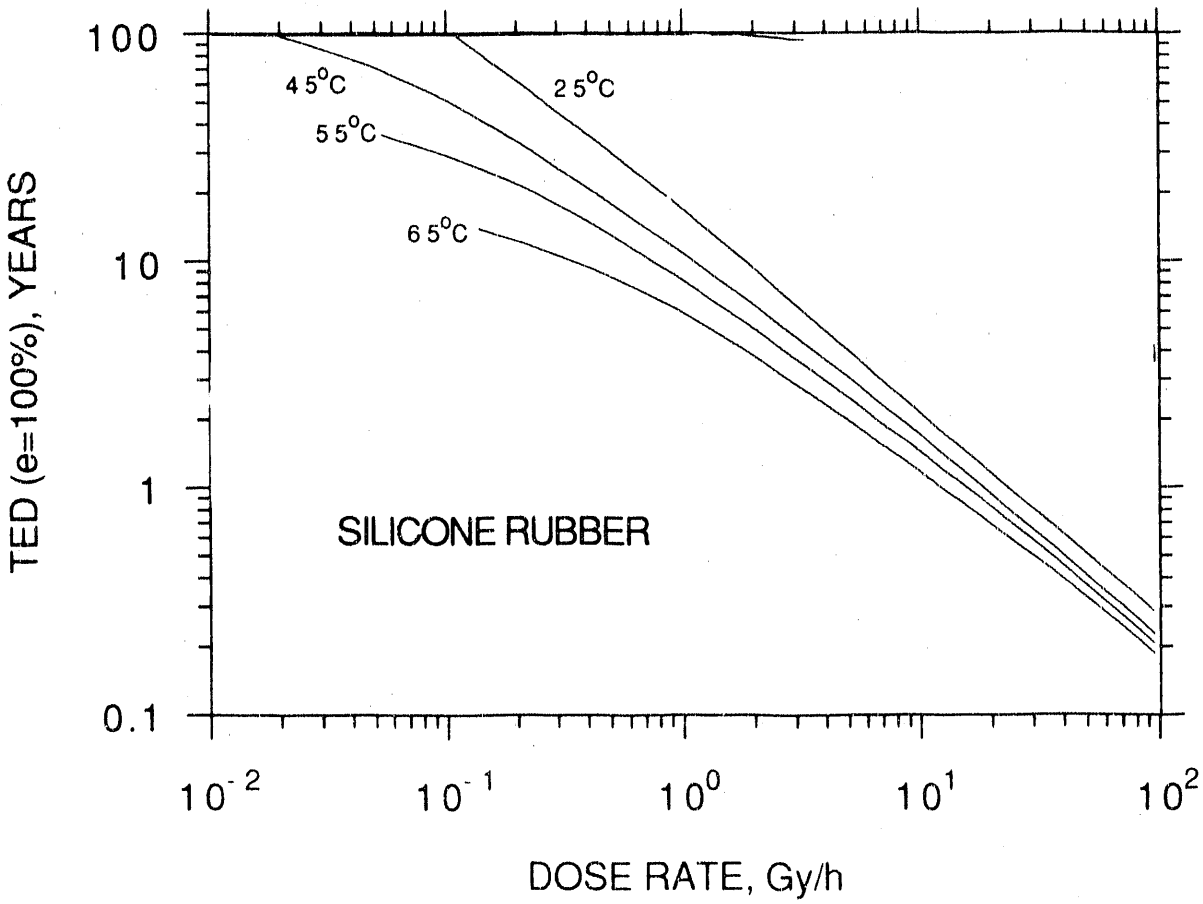

Fig. 25. Predictions for a particular commercial silicone rubber material (see Table 1) versus dose rate and temperature based on superposed model results. The time to equivalent damage (TED) refers to the predicted time required for the elongation to decrease to 100% absolute.

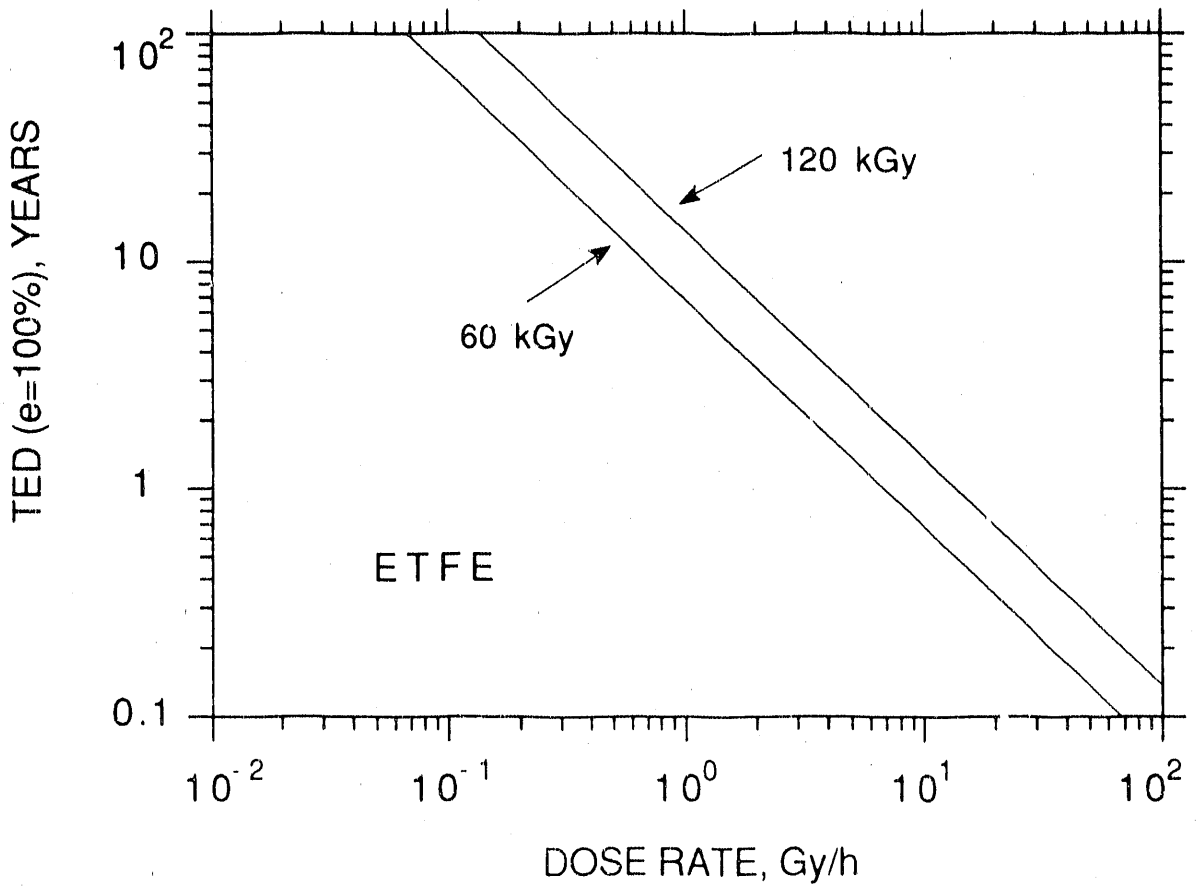

Fig. 26. ETFE predictions based on the assumption that the dose to 100% absolute elongation is 90±30 kGy, independent of the dose rate and temperature (at low to moderate temperatures).

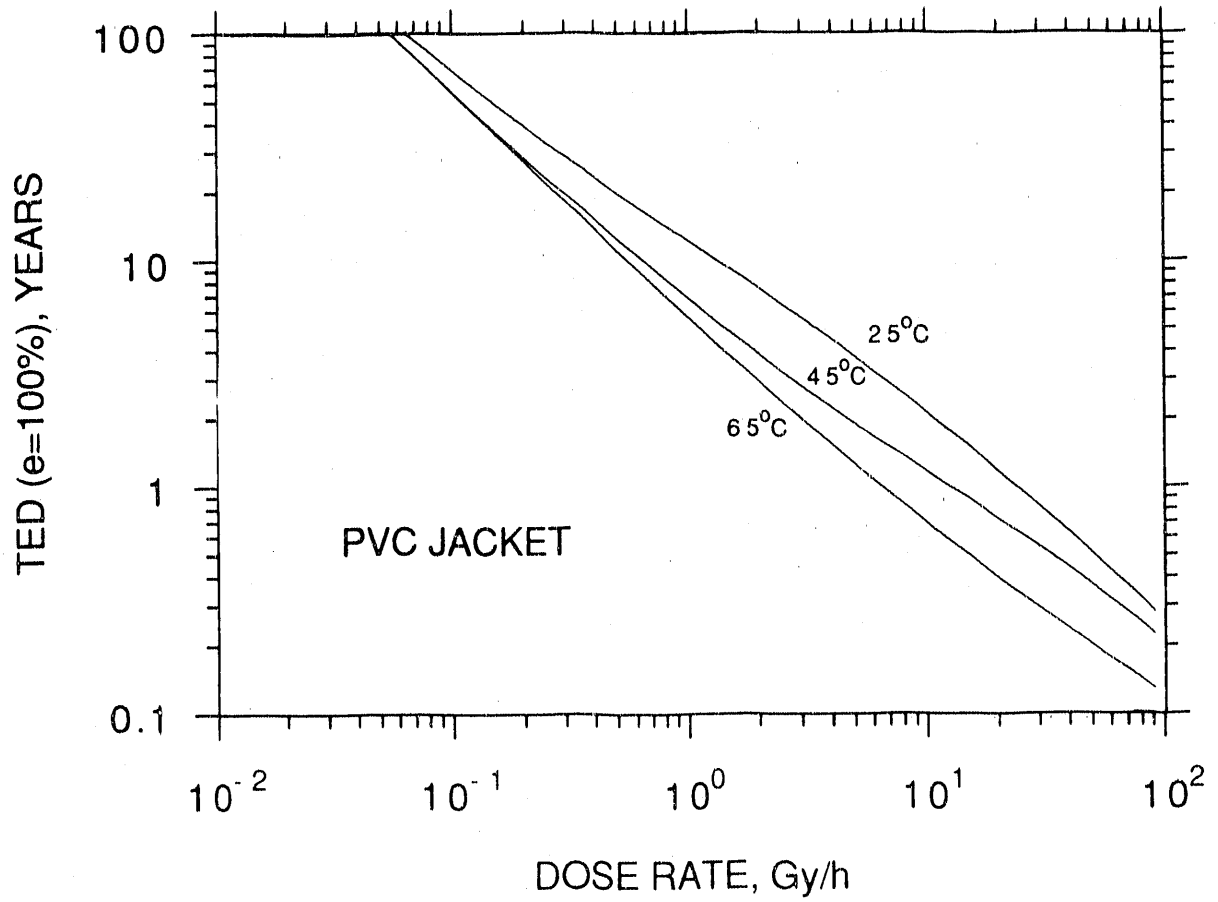

Fig. 27. Predictions for a particular commercial PVC material (see Table 1) versus dose rate and temperature based on superposed model results. The time to equivalent damage (TED) refers to the predicted time required for the elongation to decrease to 100% absolute.

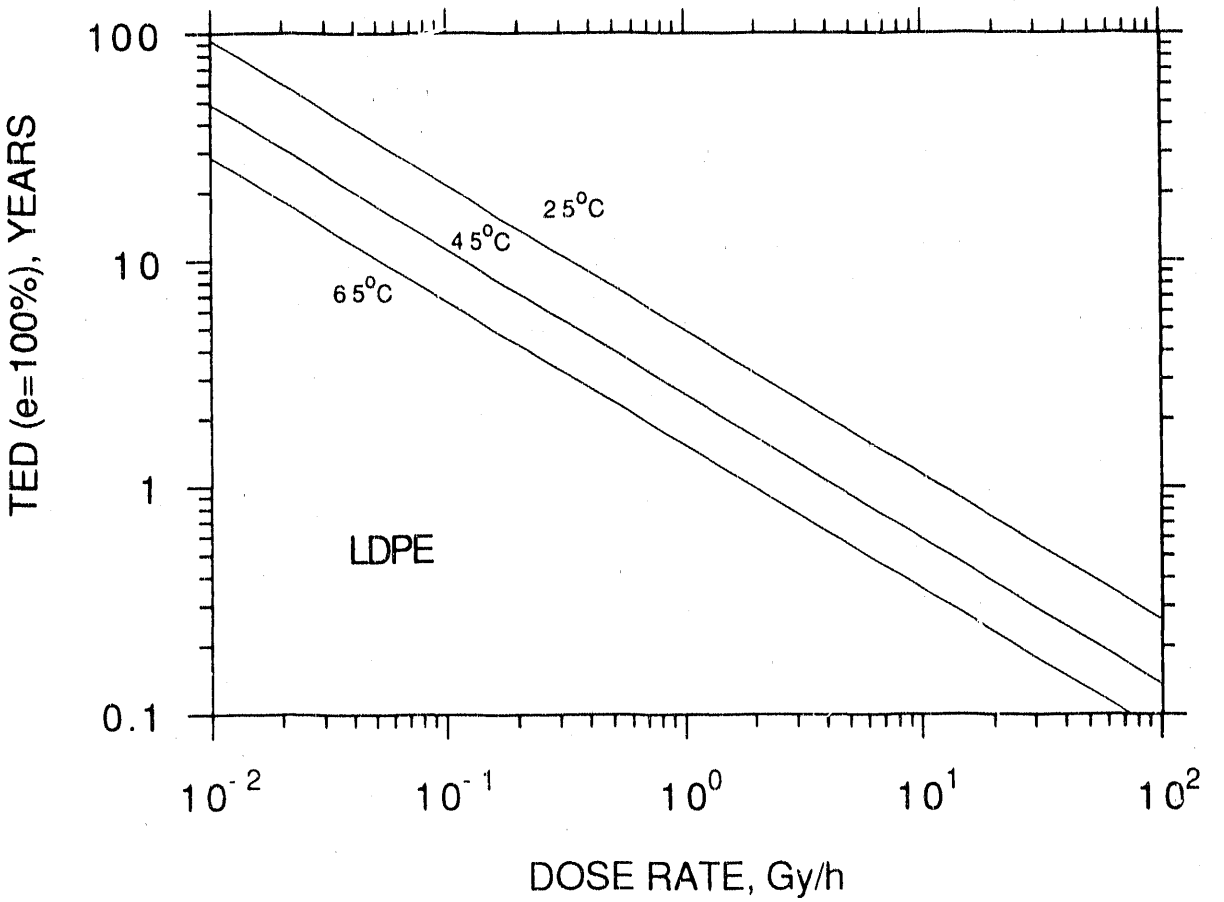

Fig. 28. Predictions for a particular commercial low density polyethylene material (see Table 1) versus dose rate and temperature based on superposed model results. The time to equivalent damage (TED) refers to the predicted time required for the elongation to decrease to 100% absolute.

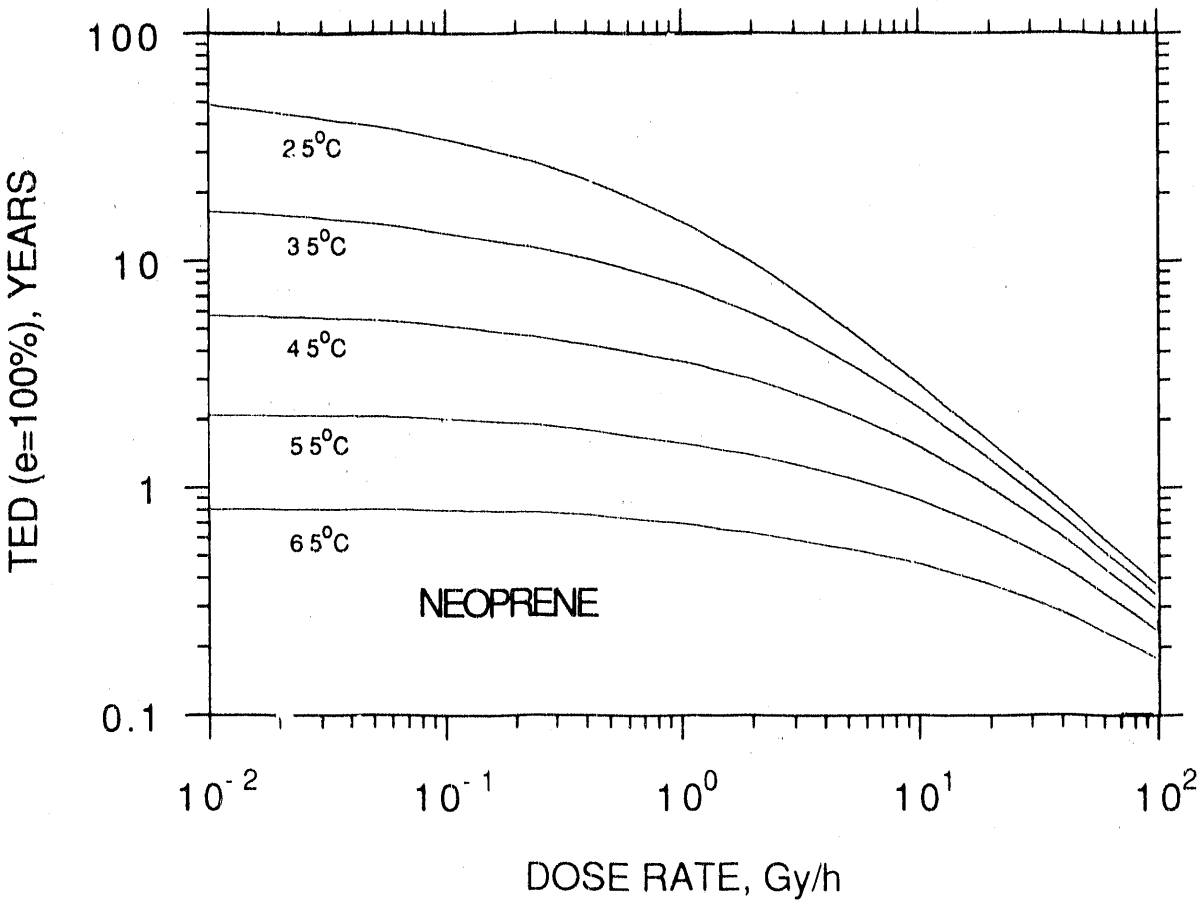

Fig. 29. Predictions for a particular commercial neoprene material (see Table 1) versus dose rate and temperature based on superposed model results. The time to equivalent damage (TED) refers to the predicted time required for the elongation to decrease to 100% absolute.

TABLE 3

Summary of Expected Dose-Rate Effects

Material	Predicted/Expected Dose to e = 100%, Gy			A/C
	at 10^4 Gy/h + ambient temp. A	at 10^2 Gy/h + 45°C B	at 0.1 Gy/h + 45°C C	
CLPE	$1x10^6$	$7x10^5$	$(7x10^5)$*	1.4
Hypalon-B	$2.5x10^6$	$1.5x10^6$	$2x10^5$	13
Hypalon-C	$1.3x10^6$	$7.5x10^5$	$8x10^4$	16
Hypalon-A	$1.4x10^6$	$8.7x10^5$	$8x10^4$	18
ETFE-B	$3x10^5$	$1.1x10^5$	$(1.1x10^5)$*	2.7
ETFE-A	$2x10^5$	$8x10^4$	$(8x10^4)$*	2.5
PVC	$1.4x10^6$	$1.9x10^5$	$5.2x10^4$	27
Silicone	$3x10^5$	$2x10^5$	$4.6x10^4$	7
LDPE	$8x10^5$	$1.2x10^5$	$1x10^4$	80
Neoprene	$4.4x10^5$	$2.5x10^5$	$4.4x10^3$	100

* Horizontal extrapolation- assumes no chemical dose-rate effect

(1) 10^4 Gy/h at ambient temperature- conditions often used for aging simulations (diffusion-limited oxidation effects are usually important),
(2) 10^2 Gy/h plus 45°C- reasonably accessible experimental conditions (diffusion effects often minimal),
(3) 0.1 Gy/h plus 45°C- may be representative of real nuclear power plant aging conditions (predictions from modelling).

The last column, which gives the approximate ratios between the first and third conditions, shows the potential impact of dose-rate effects.

To a first approximation, physical effects caused by diffusion-limited oxidation anomalies, dominate the dose-rate effects operative in going from the column marked A to the column marked B. These effects are denoted schematically in Fig. 1 by the "diffusion effects" region at high dose rates. Since the importance of diffusion effects depends on geometry (e.g., sample thickness), the high-dose-rate results (column A) apply to the material thicknesses studied (see Table 1).

Chemical dose-rate effects dominate the differences predicted between columns B and C. For the PVC, LDPE and silicone materials, these chemical dose-rate effects occur under conditions far removed from thermal-only influence and therefore correspond to the behavior schematically represented by curve III in Fig. 1. The large chemical dose-rate effects found for the neoprene and hypalon materials are due to the importance of thermal-only effects at low dose rates and therefore correspond to curve II type behavior. This thermal influence can lead to very large "dose-rate effects" in materials like neoprene, if the thermal-only environment dominates combined-environment aging.

The conditions used in column C were somewhat arbitrarily chosen. The importance of dose-rate effects under other nuclear power plant aging conditions can be estimated using the modelling results or, equivalently, Figs. 22-29.

The above discussion centered on estimating the lifetime of nuclear power plant cables. If sometime during its lifetime, a cable has to perform in a harsh accident environment, the situation becomes more complex. In general the cable would have to be preaged to a condition equivalent to its ambient lifetime aging, then tested in a simulated accident environment. If the time-temperature-dose rate superposition approach has been shown to be appropriate for a given material, it allows us to select accelerated combined-environment conditions which are equivalent to chosen ambient aging conditions. In an earlier publication [3], we showed that the equivalent conditions can be easily determined by plotting a straight line of slope equal to the shift activation energy on a graph of the log of the dose rate versus the inverse temperature in °K. Suppose, for instance, that aging conditions for safety-related cables corresponded to 45°C plus 0.1 Gy/h (a reasonable assumption, given current knowledge). If a 21 kcal/mol activation energy was appropriate for the time-temperature-dose rate

superposition of a particular material, Fig. 30 shows a plot giving the combinations of accelerated dose rate and temperature conditions which can be used to simulate these ambient conditions. The amount of acceleration is given by the ratio of the accelerated dose rate to the ambient dose rate. If a 21 kcal/mol shift activation energy is appropriate, an ambient exposure of 60 years at 0.1 Gy/h and 45°C can, for example, be simulated by 1050 h at 118°C plus 50 Gy/h or 5250 h at 96°C plus 10 Gy/h (see Fig. 30). When choosing the accelerating conditions, the usual cautionary statements must be kept in mind. First, the acceleration cannot be so high that it causes heterogeneous, diffusion-limited oxidation. Second, the temperature should not be raised above some transition of the material unless the effect of extrapolating across the transition is understood.

The situation becomes more complex for an entire cable assembly which typically involves one or more insulated conductors surrounded by one or more jackets. If different activation energies were appropriate for the different materials, one approach would be to select accelerated conditions based on the material that has the lowest activation energy. This material would then be aged equivalent to ambient while all other materials will be overaged. Based on the studies conducted to date on important cable materials used in nuclear power plant safety applications, it appears that most materials yield reasonable superposition and consistency with long-term results for activation energies ranging from ~21 to 25 kcal/mol. Therefore the generic use of 21 kcal/mol might represent a conservative approach for choosing accelerated aging conditions for a cable assembly. For example the Kerite FR cable comprises the hypalon-B insulation described above (21 kcal/mol activation energy) surrounded by the hypalon-B jacket material (24 kcal/mol) discussed in the earlier report. [3] Accelerated aging conditions for the entire cable assembly would be chosen using an analysis based on the 21 kcal/mol activation energy (e.g., Fig. 30).

When whole cables are being aged, the problem of heterogeneous effects becomes more difficult to deal with because the effective material thicknesses become larger, since oxygen must be resupplied by diffusion through the jacket and then through the insulation. This leads to the requirement of lower accelerated dose rates to avoid diffusion-limited anomalies. Estimates for hypalon based on the analysis detailed in our earlier report would indicate that the oxidative penetration distances corresponding to 50 Gy/h plus 118°C and to 10 Gy/h plus 96°C are ~1.8 mm and 2.9 mm, respectively. [3] Since the jacket of the Kerite FR cable is ~1.5mm thick, accelerated aging conditions of 10 Gy/h plus 96°C or lower would be required to reasonably assure the absence of important diffusion-limited oxidation effects. Various experimental profiling techniques [6-10] could be applied to the materials after the aging simulations to assure that the conditions selected resulted in homogeneously oxidized materials.

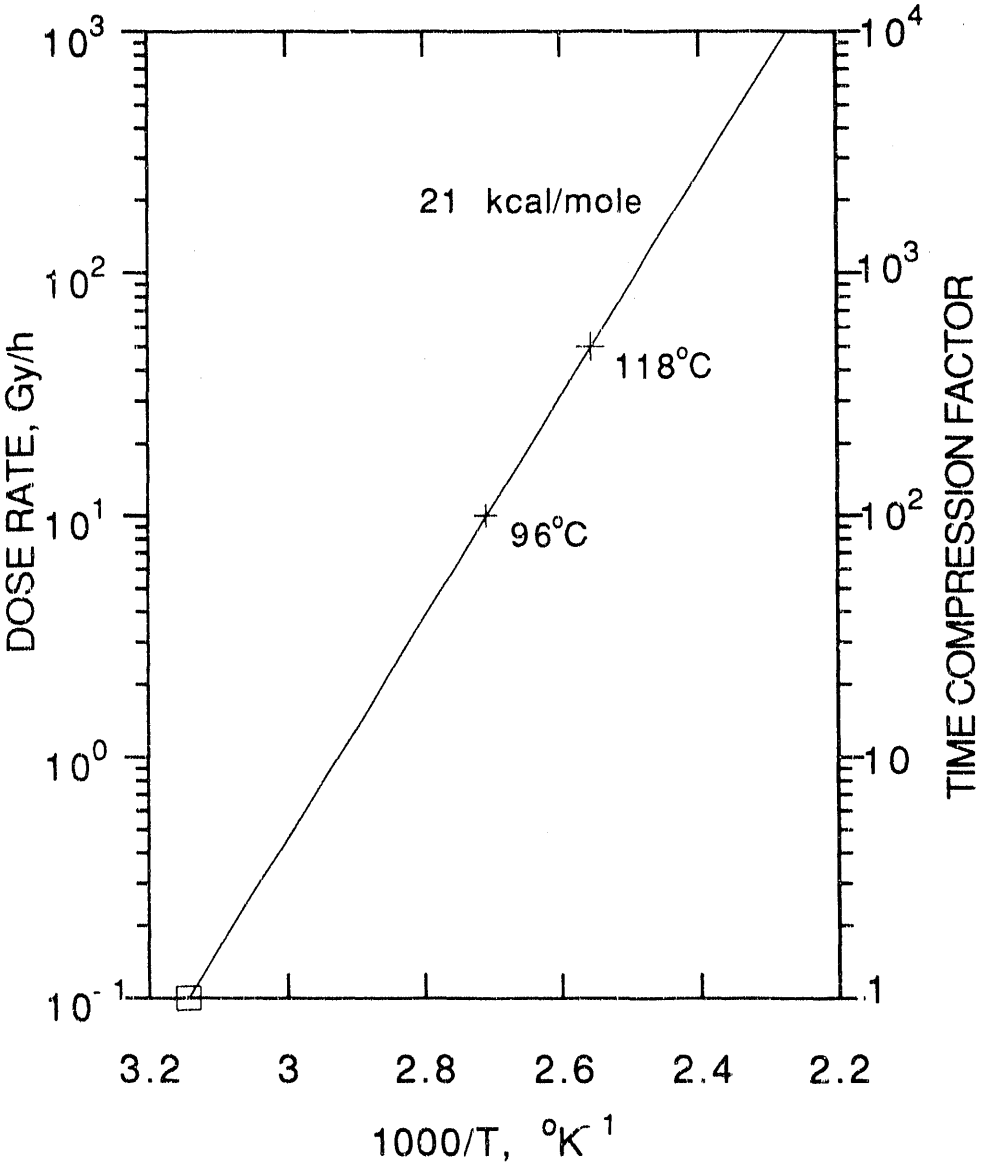

Fig. 30. Plot illustrating how accelerated combined radiation-thermal conditions equivalent to selected aging conditions can be chosen for a 21 kcal/mol activation energy dependent upon the acceleration factor desired.

REFERENCES

1. R. L. Clough, K. T. Gillen, J. L. Campans, G. Gaussens, H. Schonbacher, T. Seguchi, H. Wilski and S. Machi, Nuclear Safety 25, 238 (1984).
2. L. L. Bonzon, F. J. Wyant, L. D. Bustard and K. T. Gillen, "Status Report on Equipment Qualification Issues Research and Resolution", Sandia Labs Report, NUREG/CR-4301, SAND85-1309 (November, 1986).
3. K. T. Gillen and R. L. Clough, "Time-Temperature-Dose Rate Superposition: A Methodology for Predicting Cable Degradation Under Nuclear Power Plant Aging Conditions", Sandia Labs Report, SAND88-0754 (August, 1988).
4. K. T. Gillen, R. L. Clough and L. H. Jones, "Investigation of Cable Deterioration in the Containment Building of the Savannah River Nuclear Reactor", Sandia Labs Report, NUREG/CR-2877, SAND81-2613 (August, 1982).
5. K. T. Gillen and R. L. Clough, J. Polym. Sci., Polym. Chem. Ed., 23, 2683 (1985).
6. R. L. Clough, K. T. Gillen and C. A. Quintana, J. Polym. Sci., Polym. Chem. Ed., 23, 359 (1985).
7. K. T. Gillen, R. L. Clough and N. J. Dhooge, Polymer, 27, 225 (1986).
8. K. T. Gillen, R. L. Clough and C. A. Quintana, Polym. Degrad. and Stabil., 17, 31 (1987).
9. K. T. Gillen and R. L. Clough, "Techniques for Monitoring Heterogeneous Oxidation of Polymers", in Handbook of Polymer Science and Technology, Vol. 2, Performance Properties of Plastics and Elastomers, N. P. Cheremisinoff, Ed., Marcel Dekker, New York, 1989, Ch. 6.
10. K. T. Gillen and R. L. Clough, Polym. Eng. and Sci., 29, 29 (1989).
11 R. L. Clough and K. T. Gillen, J. Polym. Sci., Polym,. Chem. Ed., 27, 2313 (1989).
12. K. T. Gillen and R. L. Clough, Radiat. Phys. and Chem., 22, 537 (1983).
13 T. Seguchi and Y. Yamamato, "Diffusion and Solubility of Oxygen in Gamma-Ray Irradiated Polymer Insulation Materials", Japan Atomic Energy Research Institute Publication, JAERI 1299 (March, 1986).
14. K. Arakawa, T. Seguchi and K. Yoshida, Radiat. Phys. and Chem., 27, 157 (1986).
15. J. C. Reed and J. R. Perkins, "Tefzel ETFE Fluoropolymer: Temperature Rating and Functional Characterization", paper presented at the 21st International Wire and Cable Symposium, Atlantic City, N. J., December 6, 1972.
16. M. G. Noble, Power Engineering, p. 60 (July, 1976).
17. Private communication from E. C. Neumayer, United Nuclear Industries, Inc.
18. H. Rost, A. Bleier and W. Becker, "Lifetime of Cables in Nuclear Power Plants", Proceedings of the International Conference on Operability of Nuclear Systems in Normal and Adverse Environments", Lyon, France (September, 1989).

END

DATE FILMED

02 / 11 / 91